TECHNICAL NOTES

NATIONAL ADVISORY COMMITTEE FOR AERONAUTICS

No. 873

BENDING TESTS OF A MONOCOQUE BOX

By Albert E. McPherson, Walter Ramberg, and Samuel Levy
National Bureau of Standards

Washington
November 1942

NATIONAL ADVISORY COMMITTEE FOR AERONAUTICS

TECHNICAL NOTE NO. 873

BENDING TESTS OF A MONOCOQUE BOX

By Albert E. McPherson, Walter Ramberg, and Samuel Levy

SUMMARY

A monocoque box beam consisting of a 24S-T aluminum-alloy sheet reinforced by four bulkheads and by longitudinal stringers and corner posts was subjected to bending loads as follows: pure bending about the lift axis, cantilever bending about the lift axis, and pure bending about both lift and drag axes. Longitudinal strains were measured for loads up to a load at which permanent set became measurable. The loads were sufficient to produce buckling of the sheet between stringers on the compression side of the box. The only noticeable effect of this buckling was a small increase in extreme-fiber strain on the compression side. The measured strains and measured deflections differed less than 10 percent from those computed from the simple beam theory after taking account of the effective width of the buckled sheet. The effect of the bulkheads on the distribution of stringer strain was negligible.

INTRODUCTION

The bending tests of a monocoque box described in this paper are part of an investigation on monocoque boxes conducted at the National Bureau of Standards for the National Advisory Committee for Aeronautics. The purpose of this investigation is to study the stress distribution and the deformation of a monocoque box of typical design under compressive loads, bending loads, and torsional loads. The compressive tests are reported in reference 1. Torsion tests are reported in reference 2. A test to failure has not yet been made.

SPECIMEN

The over-all dimensions and the design of the monocoque box specimen are given in figure 1. A detailed description of the specimen and stress-strain graphs of the material are given in reference 1.

TESTS

Pure Bending about Lift Axis

Procedure.- The method of applying a pure bending moment about the lift axis of the monocoque box is shown in figure 2. A pair of steel booms A having a length of approximately 72 inches was rigidly fastened to the steel end plates B of the specimen. The specimen was then mounted in a vertical testing machine of 600,000-pound capacity by suspending the ends of the boom from two pairs of rods D the upper ends of which were attached to the towers E, which in turn were fastened to the bottom platen C of the testing machine. The load was applied to the end plates B of the specimen through two pairs of rods F the bottom ends of which were connected to the cross beam G, which in turn was loaded by the head H of the testing machine.

The deflection of the box under load was measured by five pairs of 0.001-inch dial micrometers mounted on a reference channel I (fig. 2) the ends of which were suspended near the ends of the specimen by a pair of flexure plates J. The rods K were placed between the spindles of the dials L and center punch marks on the corner posts at points spaced about 9.5 inches.

The strains at the stringers and at the corner posts were measured by Tuckerman optical strain gages using the technique described in reference 1. The strain gages on the top face of the box were read from the wooden platform over the specimen shown in figure 3.

The load was at first increased in steps of 18,000 pound-inches and deflections and strains were read for each load. The load was released to zero after each increase of 36,000 pound-inches in order to determine permanent set. Above 288,000 pound-inches, the load was

increased in steps of 36,000 pound-inches and after each increase the load was returned to 288,000 pound-inches to determine permanent set. Permanent set became noticeable at a load of 504,000 pound-inches. This load was chosen as an upper limit in order not to deform the specimen permanently.

Results.- The strains at the stringers and at the two corner posts on a line across the compression face at the center section of the box are shown in figure 4. The strain in the stringer at the point of contact with the sheet was calculated from the two observed stringer strains on the assumption that plane sections in the stringer remain plane. The strains across the compression face were practically uniform at all loads both before and after buckling of the sheet between stringers.

Figure 5 shows strains at four pairs of gage lines on the top center stringer. Two pairs of the gage lines were close to a bulkhead and the other two were approximately midway between bulkheads. The strain on the sheet side of the inner flange was calculated from the observed stringer strains on the assumption that plane sections in the stringer remain plane. The stringer strains were generally higher at the outer flange than at the sheet and the ratio of the strains was about the same as the ratio of the distances from the neutral fiber, 1.17. This result indicates that the simple beam theory holds approximately even after buckling of the sheet between stringers.

The strains at the corner posts are plotted against moment in figure 6. The compressive strains on the left and right exceeded the corresponding tensile strains on the left and right, respectively, for moments greater than 10,000 pound-inches by amounts that gradually increased to about 5 percent for the highest moment.

The strains at the sheet sides (inner flange) of the stringers and the strains at the tops of the outer flanges of the stringers are plotted against moment in figure 7. The strains at the sheet side of the stringers are nearly the same on the compression face as on the tension face of the box. The difference between the strains on the sheet sides and those at the tops of the outer flanges of the stringers is greater for the stringers carrying compression than for the stringers carrying tension. This result indicates that the stringers are bent more on the compression face than on the tension face of the box.

The deflection curve as indicated on the dials is shown in figure 8. The deflection curve remained a parabola throughout the tests. The center deflections relative to points $9\frac{1}{2}$ inches and $39\frac{3}{4}$ inches from the center are plotted against the load in figure 9. The center deflection was directly proportional to the load within the error of measurement.

Experimental values of the effective flexural rigidity EI were obtained by substitution of the strain readings at the corner posts (fig. 6) in

$$EI = Mh/(\epsilon_1 - \epsilon_2) \tag{1}$$

where M is the external bending moment and ϵ_1 and ϵ_2 are the strains measured at fibers that are a distance h apart. These values are plotted against the bending moment in figure 10.

Experimental values of the flexural rigidity were also obtained by substitution of the values of center deflections relative to points $39\frac{3}{4}$ and $9\frac{1}{2}$ inches from the center (fig. 9) in

$$EI = Ml^2/8d \tag{2}$$

where d is the center deflection over a span l. These values of EI are also plotted against the bending moment in figure 10.

Theoretical values of EI as a function of M were obtained as follows: Below the buckling load the moment of inertia I was computed in the usual manner from the cross-sectional dimensions as

$$I = 192 \text{ in.}^4$$

Young's modulus E was taken as an average value (see table I of reference 1)

$$E = 10.6 \times 10^6 \text{ lb/sq in.}$$

With the beginning of buckling the moment of inertia is reduced a small amount

$$\Delta I = c^2 \Delta A \tag{3}$$

where

c distance of sheet from neutral fiber, 5 inches

$$\Delta A = n(b - w)t = nbt\left(1 - \frac{w}{b}\right) \quad (4)$$

n number of sheet bays, 6

b average width of sheet between stringers, 4 inches

t sheet thickness, 0.0265 inch

w effective width of sheet between stringers

The compression test (reference 1) had shown that the effective width was in agreement with Cox's formula

$$\frac{w}{b} = 0.14 + 0.85\sqrt{\frac{\sigma_{cr}}{\sigma}} \quad (5)$$

where

σ_{cr} theoretical value of buckling stress for rigid clamping of sheet at the edges, 2880 pounds per square inch

σ edge stress which is, in this case, related to the bending moment M by $\sigma = Mc/I$

Substitution of this value in equations (3) to (5) gives

$$\Delta A = 0.547 - 180/\sqrt{M} \quad (6)$$

and

$$EI = E(I_0 - c^2\Delta A) = 10.6 \times 10^6 (192 - 25\Delta A) \quad (7)$$

Equation (7) is shown as a curve in figure 10. The computed values of EI agree closely with values obtained from the observed strains measured at the corner posts. They agree, within the accuracy of measurement, with the points determined by deflection measurements.

The strains in the inner and the outer flange of the Z-stringers were calculated from

$$\epsilon_y = My/EI \quad (8)$$

where ϵ_y is the compressive strain for a fiber at a distance y from the neutral fiber of the box (y taken as positive on the compression side). Above the buckling load the loss in effective width of sheet on the compression face causes the neutral fiber to shift, so that

$$y = y_0 + c\Delta A/A \tag{9}$$

where

y_0 distance to neutral fiber before buckling

$c\Delta A/A$ shift in neutral fiber due to buckling

A cross-sectional area of box, 8.46 square inches

Substitution of (9) and (7) in (8) gives

$$\epsilon_y = \epsilon_{y_0}\left[1 + \frac{\Delta A}{A}\left(\frac{c}{y_0} + c^2\frac{A}{I_0}\right)\right]. \tag{10}$$

where $\epsilon_{y_0} = \frac{My_0}{EI_0}$ and denotes the strain in the absence of buckling.

Substitution of the given numerical values and $y_0 = \pm 5.04$ inches and $y = \pm 5.89$ inches for the inner and the outer flanges of the stringers, respectively, gives the curves shown in figure 7. The measured strains for the flanges of the stringers on the compression face of the box are in close agreement with the calculated strains; the other measured strains are greater than the calculated strains by amounts that approach 10 percent at the highest loads.

Cantilever Bending about Lift Axis

Procedure.- The monocoque box was subjected to cantilever bending about the lift axis by loading it, as shown in figures 11 and 12. In order to achieve this loading, one of the booms A in figure 2 was removed. A downward load F was applied by the head H of the testing machine and this load was balanced by the reaction P at the left end of the specimen and D at the end of the

boom on the right of the specimen. These loads subjected the monocoque box to a constant vertical shearing force P and a bending moment that increased linearly from zero at the left end of the specimen to a maximum at the right end.

Deflections and strains were measured as for the previous test. Figure 13 shows the method of attaching strain gages to read strains at the center section of the box. Permanent set became noticeable at a load of 14,000 pounds. This load was therefore chosen as an upper limit to the loads applied to the specimen.

Results.- Strains were read at five sections normally 42, 49, 57, 62, and 70 inches from the line of loading P at the free end of the box. The results for the five stringers on the top face of the box are given in figures 14 to 18. The strains varied linearly with the distance from the line of loading P at the end of the box except for irregular deviations of less than 4 percent. The deviations show no systematic decrease in strain in going from the corner posts to the center stringer, such as would be expected from shear lag. Strain readings were checked by repeating the tests at some locations. The check values in no case differed more than 3 percent from the original values.

Stringer strains at a section near a bulkhead and a section midway between bulkheads are shown in figures 19 and 20, respectively.

The strains are generally higher on the outer flange than on the inner flange. The ratio of the strains is about the same as the ratio of the distances from the neutral fiber, 1.16.

The centroidal strain for the bottom stringer and the average of the centroidal strains for the five top stringers are plotted against the load for the five sections in figure 21. The strains increase linearly with the load up to a strain of about 0.00025. This strain approximates the theoretical strain of about 0.00027 for buckling of a long sheet 0.026 inch thick clamped by stringers spaced 4 inches (see table 35, p. 345, reference 3). The observed strains agree closely with those calculated from equation (10) except in the case of the strain observed on the tension side at the center stringer. At the maximum load, this strain exceeded the calculated strain by 7 percent.

The corresponding data for the strain in the corner posts are shown in figure 22 for the center section of the box. Strains calculated from equation (10) are shown for comparison with the measured values. Calculated and measured strains agreed within 2 percent at all loads. There is a break in the curve through the points at a strain of about 0.00027 corresponding to buckling of the sheet on the compression side.

The deflection curve relative to points on the beam $10\frac{1}{2}$ inches in from each end is given in figure 23. Points $10\frac{1}{2}$ inches in were chosen to avoid the effects of the end reinforcements. The shape of the deflection curve corresponds to that for a cantilever beam computed from

$$\frac{y}{d} = \frac{8}{3(1 - 2a/l)^2}\left[\frac{a}{l}\left(\frac{a}{l} - 1\right) + \left(1 - \frac{a}{l} + \frac{a^2}{l^2}\right)\frac{x}{l} - \frac{x^3}{l^3}\right] \qquad (11)$$

where

y deflection at a point a distance x from the free end of the beam relative to a line through points a distance a from the load points

d center deflection $\left[y(l/2)\right]$

l length of beam between load points

and

$$a = 10.5 \text{ in.}$$

$$l = 100 \text{ in.}$$

The measured points show the same shape of deflection curve for loads above 2500 pounds as for smaller loads, although buckling of the sheet on the compression side became noticeable at a load of about 2500 pounds.

The center deflection relative to a line through points $10\frac{1}{2}$ inches from the ends of the box is plotted against end load in figure 24. The deflection increases almost linearly with the load with a slope $P/d = 50{,}000$ pounds per inch, showing that the buckling of the sheet was not sufficient to lessen appreciably the flexural rigidity. The slope P/d was substituted in the equation for center deflection,

$$d = \frac{Pl^3}{16EI}\left(1 - \frac{2a}{l}\right)^2 \qquad (12)$$

obtained from the simple beam theory. The resulting experimental value of EI is

$$EI = 198.7 \times 10^6 \text{ lb-in.}^2$$

This value differs less than 2 percent from the value for no buckling given in figure 10 and less than 1/2 percent from the average value in figure 10.

Pure Bending about Both Lift and Drag Axes

Procedure.- The monocoque box was subjected to pure bending moments about both lift and drag axes by loading it as shown in figure 25. The test differed from that illustrated in figure 2 only in having the box rotated through an angle of 18.43° with respect to the load lines. The moment about the lift axis was, therefore

$$M_L = M \cos 18.43^\circ = 0.9487\ M \qquad (13)$$

and the moment about the drag axis was

$$M_D = M \sin 18.43^\circ = 0.3162\ M \qquad (14)$$

The ratio of the moment about lift axis to the moment about the drag axis was $0.9487\ M/0.3162M = 3$.

Deflections and strains on the outstanding flanges were measured as for the previous tests. A somewhat different technique was used, however, for holding down the lever transfers and for preventing these transfers from tipping on the inclined face of the box. Force was applied to the top of the transfers by a rubber band attached to a clip, which was cemented to the box at a rivet head. The transfers were held perpendicular to the face of the box by a long thread. Figure 26 shows at I the reference bars from which the lateral deflections were measured and at J, one of the flexure plates supporting the reference bars. Tuckerman strain gages and a lever transfer for reading the strain in the bottom center stringer are shown at K. These gages had 90°

prisms attached to allow reading from the side of the specimen. Permanent set became noticeable at a load of 14,500 pounds. This load was therefore chosen as an upper limit for the loads applied to the specimen.

Results.- Strains were determined at the center section of the specimen. The results for the five stringers on the top face of the box, the corner posts, and the center stringer on the bottom face of the box are given in figures 27 and 28. The strain in the stringer at the point of contact with the cover sheet was calculated from the two measured stringer strains on the assumption that plane sections in the stringer remain plane. The strains across the top and the bottom of the box deviated from linearity by less than 4 percent for the top (compression) face and by less than 6 percent for the bottom (tension) face. Buckling of the compression face started in the top corner at a moment of 72,000 pound-inches and had spread to the region between stringer 5 and the other corner of the box at a moment of 108,000 pound-inches. The buckling did not cause a noticeable change in the strain distribution.

The strains in the corner posts are plotted against moment in figure 29. The compressive strains exceeded the corresponding tensile strains at all loads by about 8 percent. All the corner post strains increased linearly with the moment.

The measured strains in the stringers are plotted against moment in figure 30. The strains increased linearly with the bending moment. The buckling moment (about 50,000 lb-in.) was too low to indicate a measurable change in slope of the strain-moment curves of figures 29 and 30.

The location of the line of zero strain (neutral axis) was determined on the assumption that the strain varies linearly between points on the center section. The location of the axis at the maximum applied moment (M = 522,000 lb-in.) is given in figure 31. The location of the neutral axis was determined from the observed strains by the method of least squares. Buckling of the compression face caused a shift downward of the neutral axis of 0.40 inch; moments about the drag axis one-third as large as the moments about the lift axis caused the neutral axis to rotate about 2.6° with respect to its position for moments about the lift axis alone.

The deflection curve normal to the lift axis as indicated on the dials is shown in figure 32. Center deflections normal to both the drag and the lift axes were also measured (fig. 33). The ratio of the deflections with respect to the lift and the drag axes indicates (fig. 33) that the box bent about an axis inclined about 3° with respect to the lift axis. Additional measurements normal to this new axis (neutral axis) were therefore made (fig. 34). The deflection about either the lift axis or the neutral axis approximates a parabola at all bending moments (figs. 32 and 34). The center deflection (fig. 33) is directly proportional to the moment.

Experimental values for the effective flexural rigidities $(EI)_L$ and $(EI)_D$ about lift and drag axes, respectively, were obtained from the strain readings at the corner posts (fig. 29), on the assumption that plane sections remained plane, by substitution in equation (1). The values obtained are plotted against the total bending moment in figure 35.

Additional experimental values of the flexural rigidity about the lift and drag axes were obtained by substituting in equation (2) the values of the center deflection relative to points 28½ inches from the center plotted in figure 33. These values of $(EI)_L$ and $(EI)_D$ are also plotted against the total bending moment in figure 35. The large scatter in the points thus obtained for $(EI)_D$ is due to the difficulty of accurately measuring the small displacements normal to the drag axis.

The twist between sections 12 and 27 inches from the transverse center line of the box was measured using the method described in reference 2. The twist measurements were made on the diagonally opposite, most heavily stressed corner posts. One of the twist gages is shown at L in figure 26. The twist was 2×10^{-5} radians per inch on the compression corner post and 0.5×10^{-5} radian per inch on the tension corner post for a moment of 522,000 pound-inches. These twists are too small to be significant.

Theoretical values of $(EI)_L$ and $(EI)_D$ as a function of M were obtained as follows. Below the buckling moment the moments of inertia were computed in the usual manner from the cross-sectional dimensions as

$$I_{L_0} = 192 \text{ in.}^4 \qquad I_{D_0} = 937 \text{ in.}^4$$

Young's modulus E was taken as an average value (see table I of reference 1):

$$E = 10.6 \times 10^6 \text{ lb/sq in.}$$

With the beginning of buckling the moment of inertia is reduced. The compression test (reference 1) had shown the effective width to be in agreement with Cox's formula (equation (5)). In the present case the buckled sheet is not uniformly compressed because of the fact that both lift and drag moments are present. An approximation to the effective area for this case was obtained by considering the effective area dA of strips of width dx of the sheet a distance x from the drag axis, on the assumption that the relation between dA and axial stress σ in the strip was given by Cox's formula:

$$\left.\begin{aligned} dA &= td\,x\left(0.14 + 0.85\sqrt{\sigma_{cr}/\sigma}\right) && \sigma > \sigma_{cr} \\ dA &= td\,x && \sigma \leq \sigma_{cr} \end{aligned}\right\} \quad (15)$$

where

σ_{cr} theoretical value of buckling stress for rigid clamping of the sheet at the edges, 2880 pounds per square inch

and

$$\sigma = \frac{5M_L}{I_L} + \frac{xM_D}{I_D}$$

which corresponds to the usual formula $\sigma = Mc/I$. Equation (15) combined with equations (13) and (14) reduces to

$$\left.\begin{aligned} dA &= tdx\left(0.14 + \frac{45.6}{\sqrt{M}}\sqrt{\frac{I_L\, I_D}{4.743I_D + 0.3162\, I_L x}}\right) && \sigma > \sigma_{cr} \\ dA &= tdx && \sigma < \sigma_{cr} \end{aligned}\right\} \quad (16)$$

and

$$(EI)_L = E\left[I_{L_0} - \int_{-12}^{+12} S^2 (t\,dx - dA)\right] \qquad (17)$$

where S is the distance of sheet from lift axis.

$$(EI)_D = E\left[I_{D_0} - \int_{-12}^{+12} x^2 (t\,dx - dA)\right] \qquad (18)$$

Equations (17) and (18) are shown as curves in figure 35 using $E = 10.6 \times 10^6$ pounds per square inch. The calculated stiffness agreed with the measured stiffness within the error of measurement. The calculated decrease in stiffness due to buckling of the sheet was too small to be indicated by the measurements.

The neutral axis rotated owing to the moment about the drag axis, which was one-third the moment about the lift axis. The magnitude of this rotation with respect to the position of the neutral axis with moment about the lift axis alone is given by the formula

$$\theta = \frac{M_D (EI)_L}{(EI)_D M_L} \qquad (19)$$

When $M_L = 3 M_D$ this equation reduces to

$$\theta = \frac{1}{3} \cdot \frac{(EI)_L}{(EI)_D} \qquad (20)$$

At the highest moment used, M = 522,000 pound-inches, the values of $(EI)_L$ and $(EI)_D$ are given in figure 35 as

$$(EI)_L = 196 \times 10^7 \text{ lb-in.}^2$$

$$(EI)_D = 984 \times 10^7 \text{ lb-in.}^2$$

Substitution of these values in equation (20) gives

$$\theta = 0.0664 \text{ radian} = 3.8^\circ$$

This value is somewhat larger than the measured value of 2.6°.

An estimate of the shear-lag effect for the cantilever bending test about the lift axis was made by Mr. Paul Kuhn of the Langley Memorial Aeronautical Laboratory of the National Advisory Committee for Aeronautics as follows:

The shear-lag parameter is found from

$$K^2 = \frac{Gt}{Eb_s}\left(\frac{1}{A_F} + \frac{1}{A_L}\right) = \frac{0.385 \times 0.026}{7.20}\left(\frac{1}{1.14} + \frac{1}{0.64}\right) = 0.0034$$

or $K = 0.058$

The shear-lag effect increases toward the root. The strain-gage station closest to the root was $x = 30$ inches from the root, therefore

$$Kx = 1.74 \quad \text{and} \quad KL = 5.65$$

In a box of uniform section loaded at the tip, the ratio of average stringer stress to Mc/I stress is given by formula (A-7) of reference 4 as

$$R = 1 + \frac{\sinh Kx}{Kx \cosh KL} = 1 + \frac{2.76}{1.74 \times 142} = 1.01$$

The shear-lag effect is therefore about 1 percent, which is overshadowed by the accidental errors indicated by the dissymmetry of the experimental curve of chordwise distribution of stress.

CONCLUSIONS

When the monocoque box was tested within the elastic range by pure bending about the lift axis, the strains across the compression face were practically uniform at all loads both before and after buckling of the sheet between stringers. The effect of the bulkheads on the stringer strain distribution was negligible. The strains in the stringer flanges indicated that, even after buckling of the sheet, plane sections of the box remained

plane. The deflection curve remained a parabola throughout the tests and the center deflection was directly proportional to the load. Experimental values of the flexural rigidity EI determined from strain-gage readings and center-deflection measurements agreed with theoretical values within the accuracy of measurement. Measured stringer strains differed less than 10 percent from computed strains after correction for shift in neutral axis due to buckling of the sheet.

When the monocoque box was tested within the elastic range by cantilever bending about the lift axis the stringer strains varied linearly with the distance from the end load within 4 percent. There was no measurable shear lag. Observed and calculated stringer strains agreed within 7 percent. Observed and calculated corner post strains agreed within 2 percent. The shape of the deflection curve coincided with that of a cantilever beam of uniform section for all loads. The center deflection increased almost linearly with the load showing that buckling of the sheet was not sufficient to lower appreciably the flexural rigidity. The experimental value of EI determined from center deflection measurements was about 2 percent less than the value computed for no buckling, a difference of less than 1/2 percent from the average value for pure bending including buckling.

When the monocoque box was tested by pure bending about both lift and drag axes ($M_D = 1/3\ M_L$) the strains across the faces of the box differed from linearity by less than 4 percent for the compression face and 6 percent for the tension face. Buckling of the compression face did not cause a noticeable change in the strain distribution. The corner-post strains increased linearly with the moment and the compressive strains exceeded the tensile strains at all loads by about 8 percent. The stringer strains increased linearly with the moment. The strain-moment curve showed no change in slope at the buckling load of the sheet. At the highest moment measured, buckling of the compression face caused a shift downward of the neutral axis of 0.40 inch and the application of moments about both axes caused the neutral axis to rotate 2.6° with respect to the lift axis. The deflection curve was a parabola. Experimental values of the flexural rigidity about the two axes determined from the corner-post strains differed less than 10 percent from computed values. Values of flexural rigidity about the lift axis

determined from center deflection measurements differed less than 5 percent from computed values.

National Bureau of Standards,
Washington, D. C., July 10, 1942.

REFERENCES

1. Ramberg, Walter; McPherson, Albert E., and Levy, Sam: Compressive Tests of a Monocoque Box. T.N. No. 721, NACA, 1939.

2. Levy, Samuel, McPherson, Albert E., and Ramberg, Walter: Torsion Test of a Monocoque Box. T.N. No. 872, NACA, 1942.

3. Timoshenko, S.: Theory of Elastic Stability. McGraw-Hill Book Co., Inc., 1936.

4. Kuhn, Paul: Approximate Stress Analysis of Multi-stringer Beams with Shear Deformation of the Flanges. Rep. No. 636, NACA, 1938.

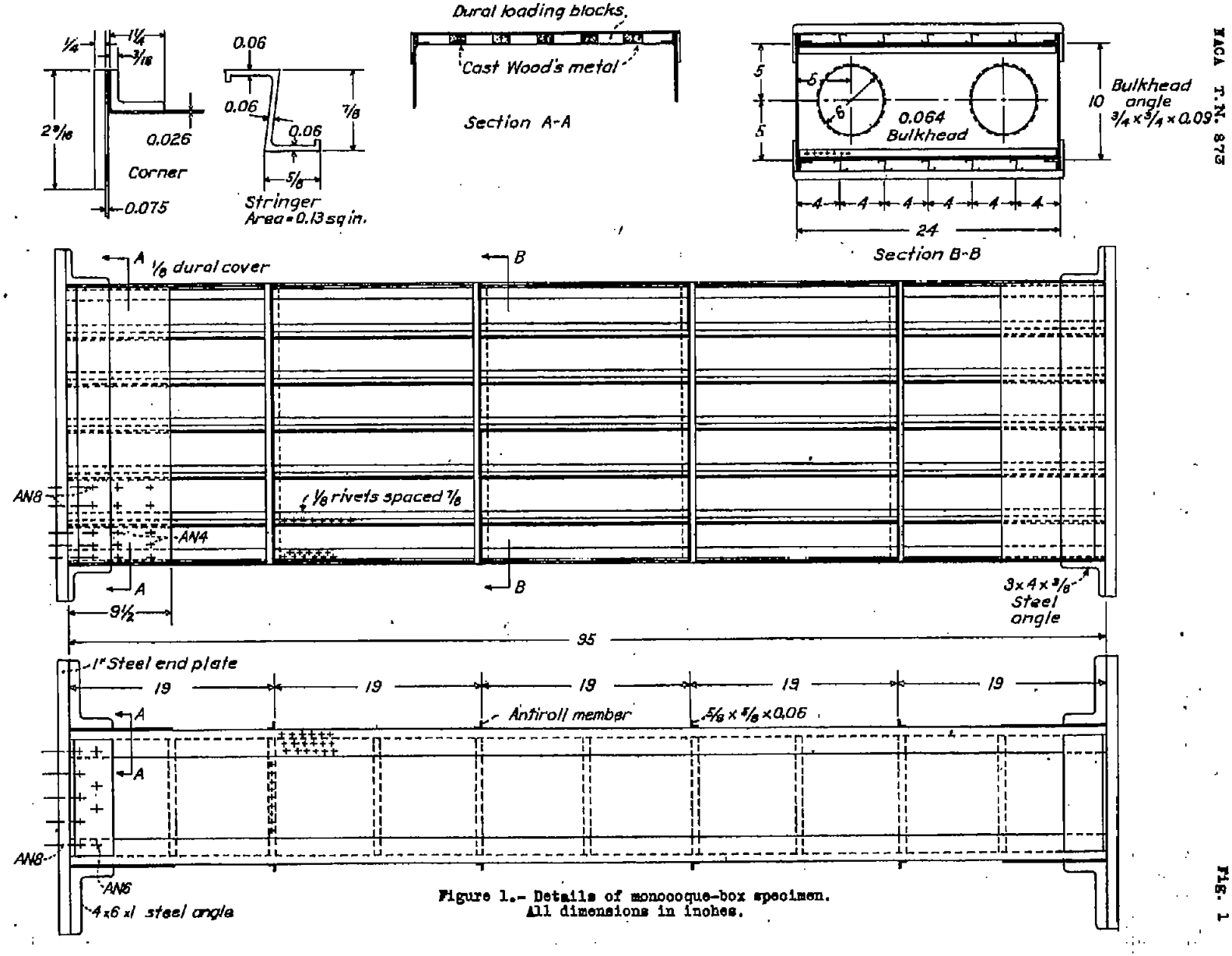

Figure 1.- Details of monocoque-box specimen.
All dimensions in inches.

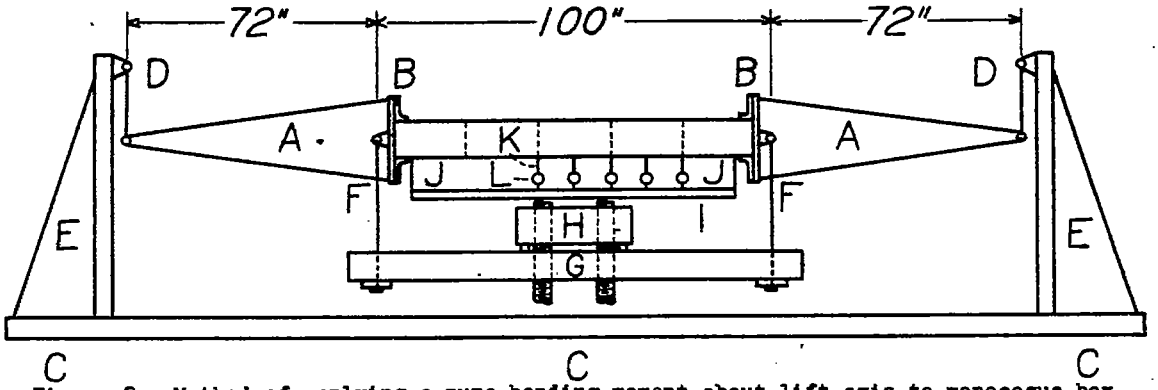

Figure 2.- Method of applying a pure bending moment about lift axis to monocoque-box specimen.

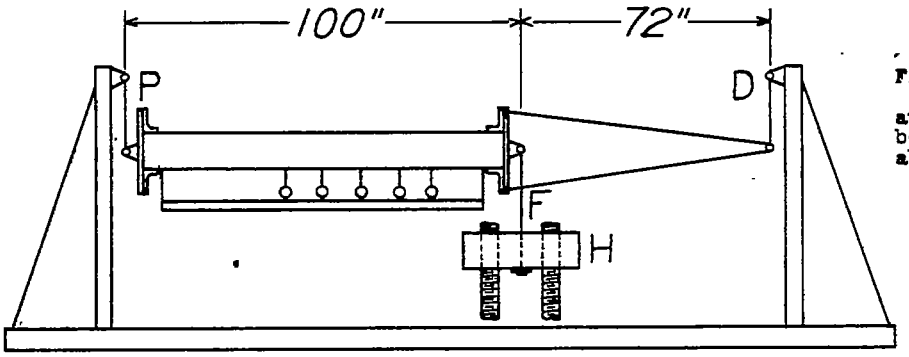

Figure 11.- Method of applying cantilever bending moment about lift axis.

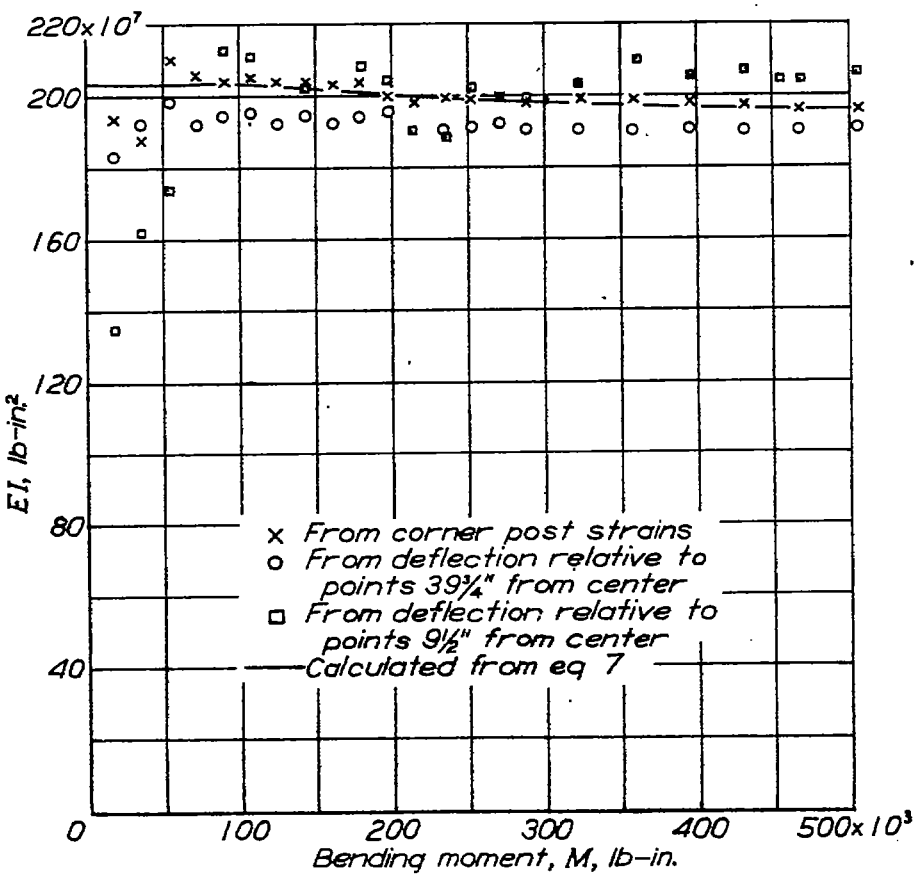

Figure 10.- Variation of effective flexural rigidity EI with bending moment.

Figure 3.- Pure bending about lift axis of monocoque box specimen.

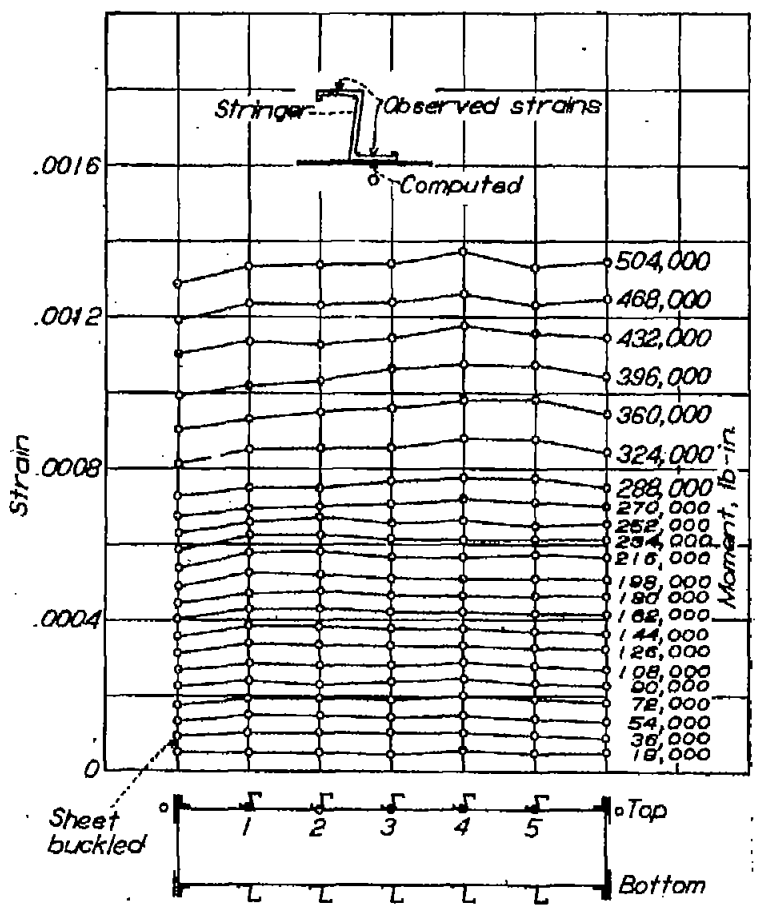

Figure 4.- Strains at stringers and at two corner posts on a line across the compression face at the center section of the box for pure bending about lift axis. Strains computed on assumption that plane sections in stringer remain plane.

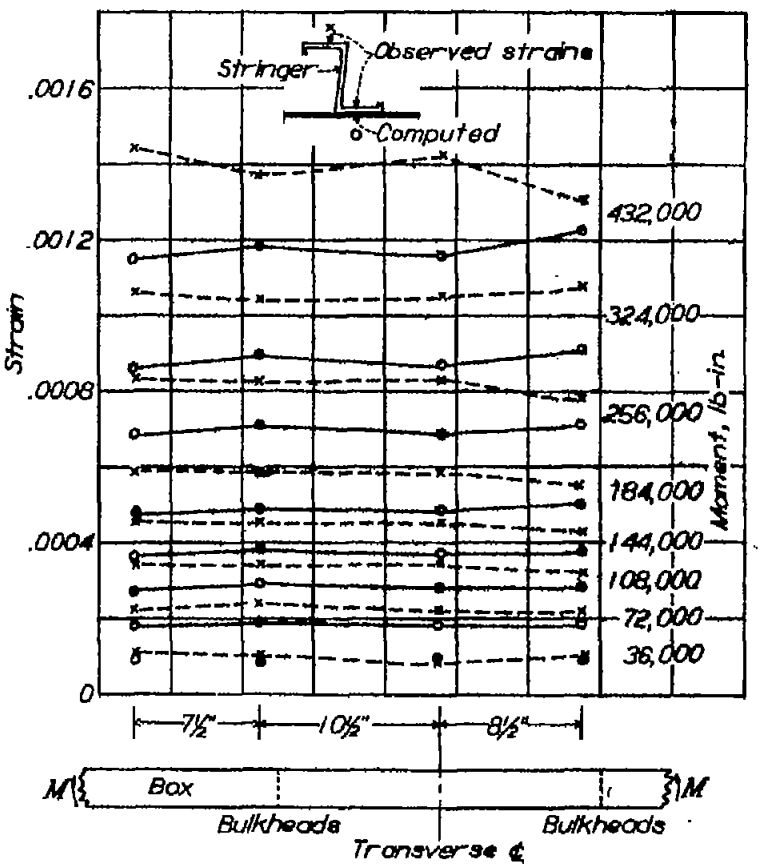

Figure 5.- Variation of strain along center stringer on compression face of box.

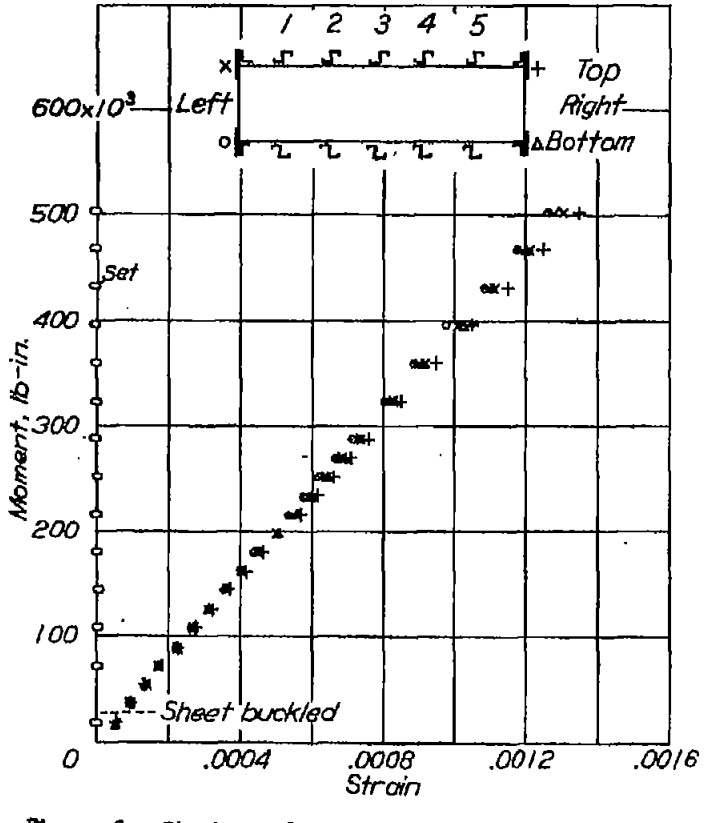

Figure 6.- Strains and permanent sets at corner posts at center section for pure bending.

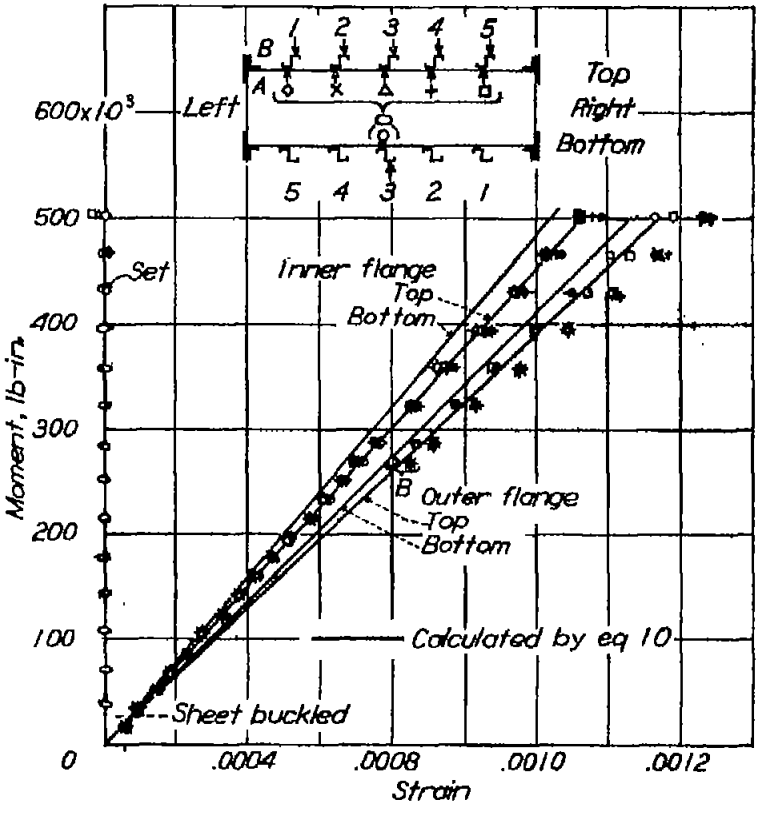

Figure 7.- Strains at sheet sides and at tops of the outer flanges of stringers.

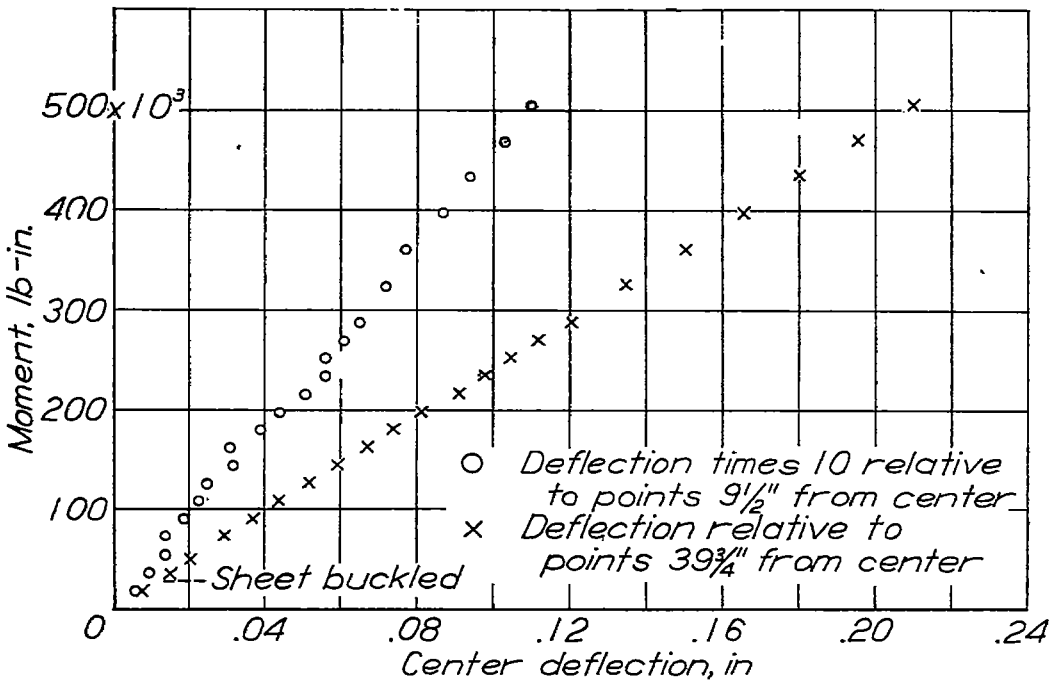

Figure 8.- Center deflection relative to points 9 1/2 and 39 3/4 inches from center.

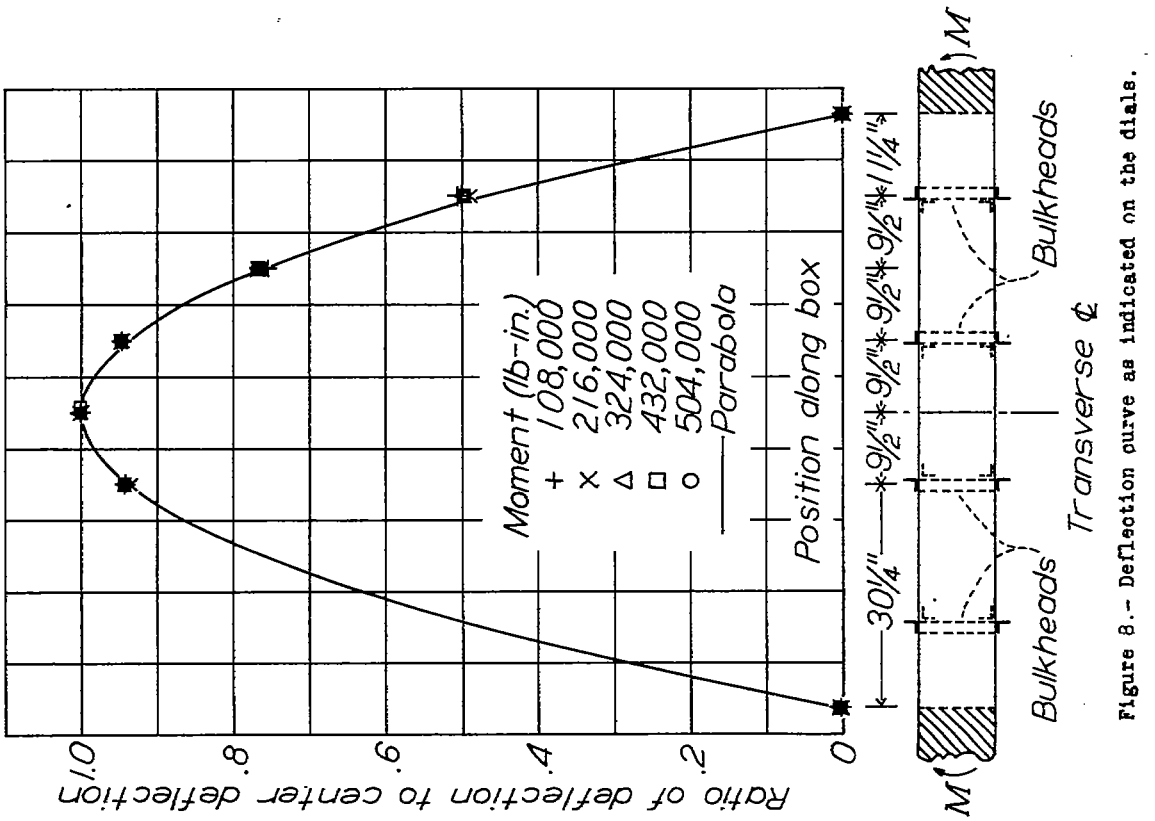

Figure 8.- Deflection curve as indicated on the dials.

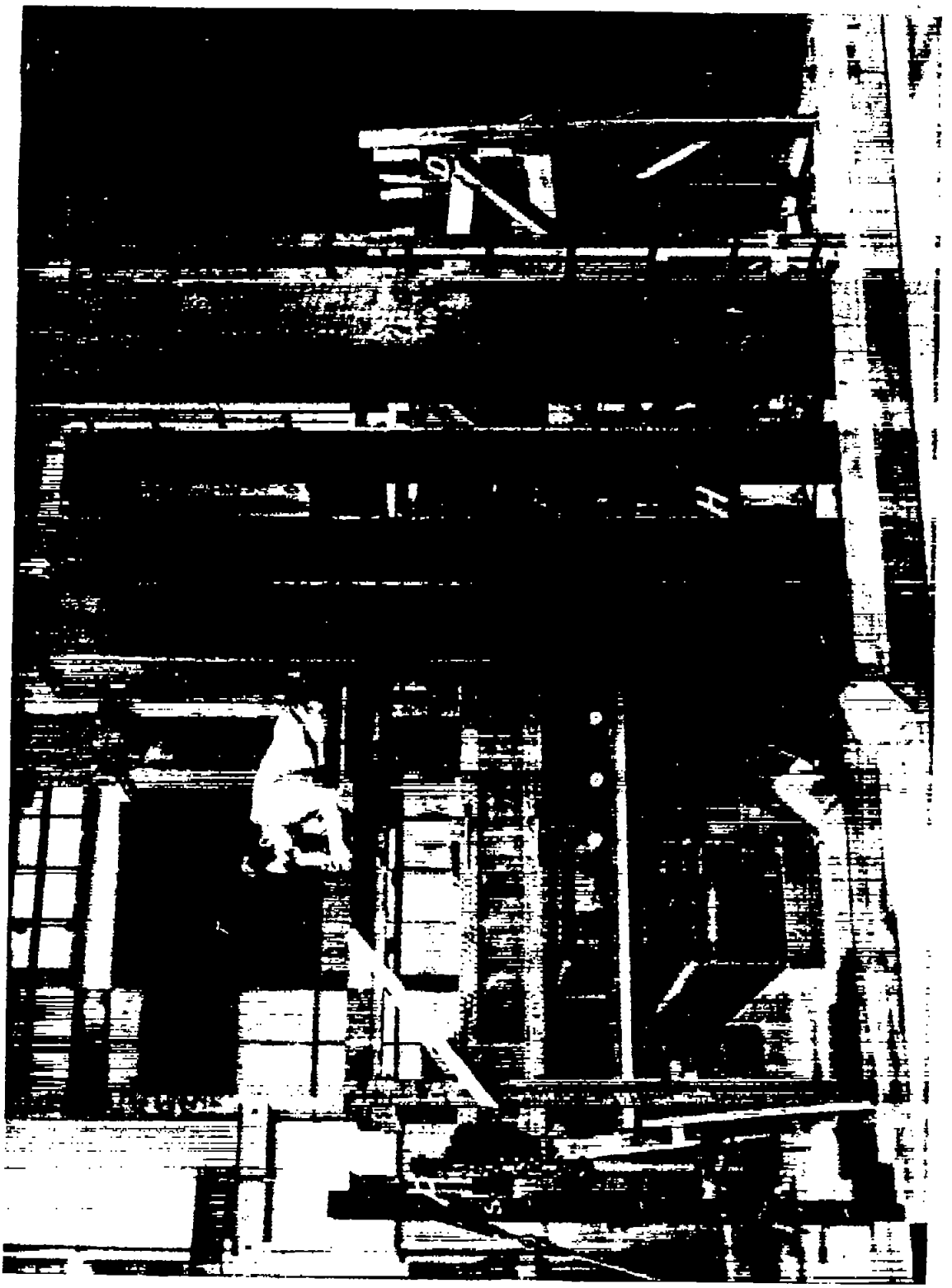

Figure 12.- Cantilever bending test of monocoque box.

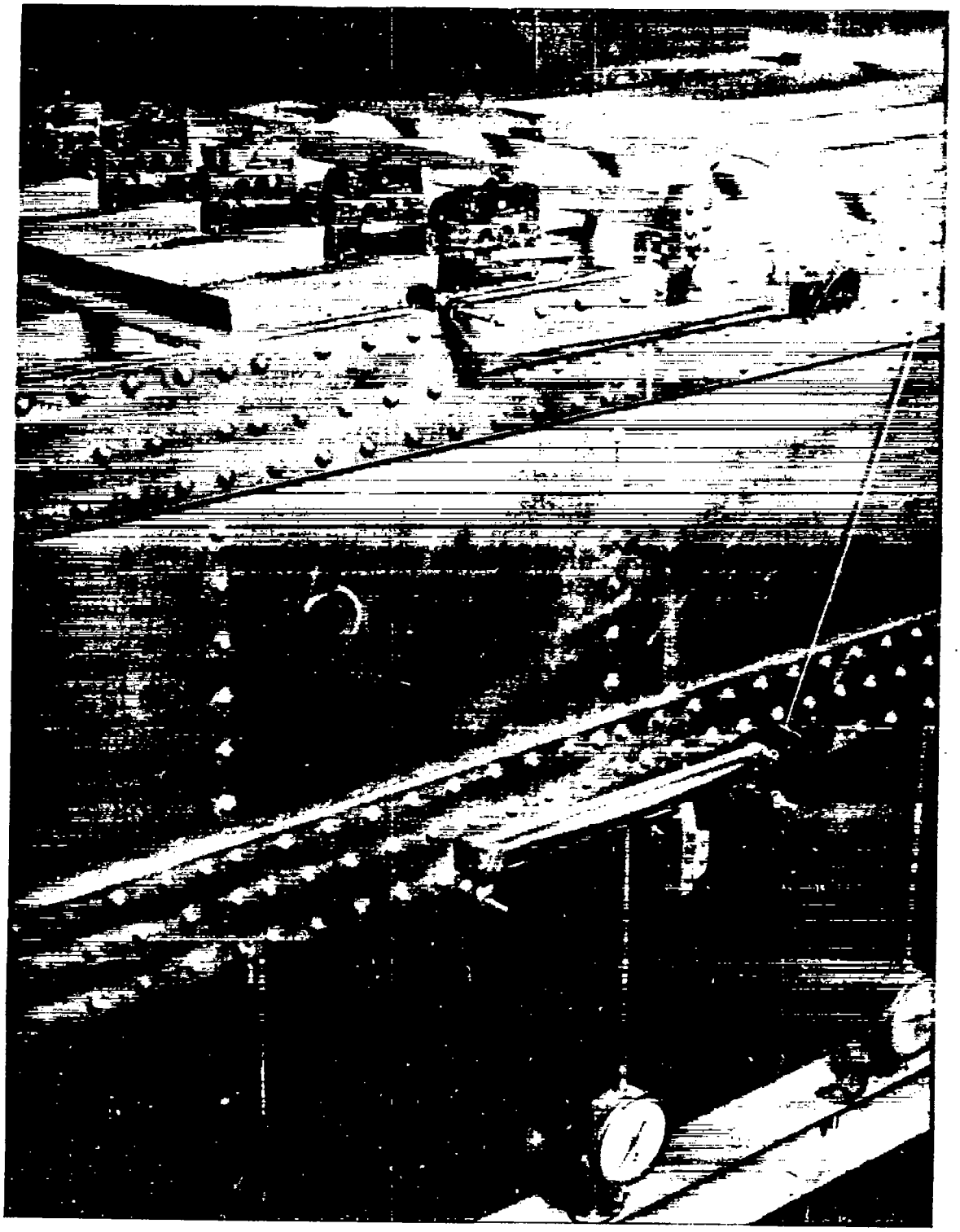

Figure 13.- Method of attaching strain gages.

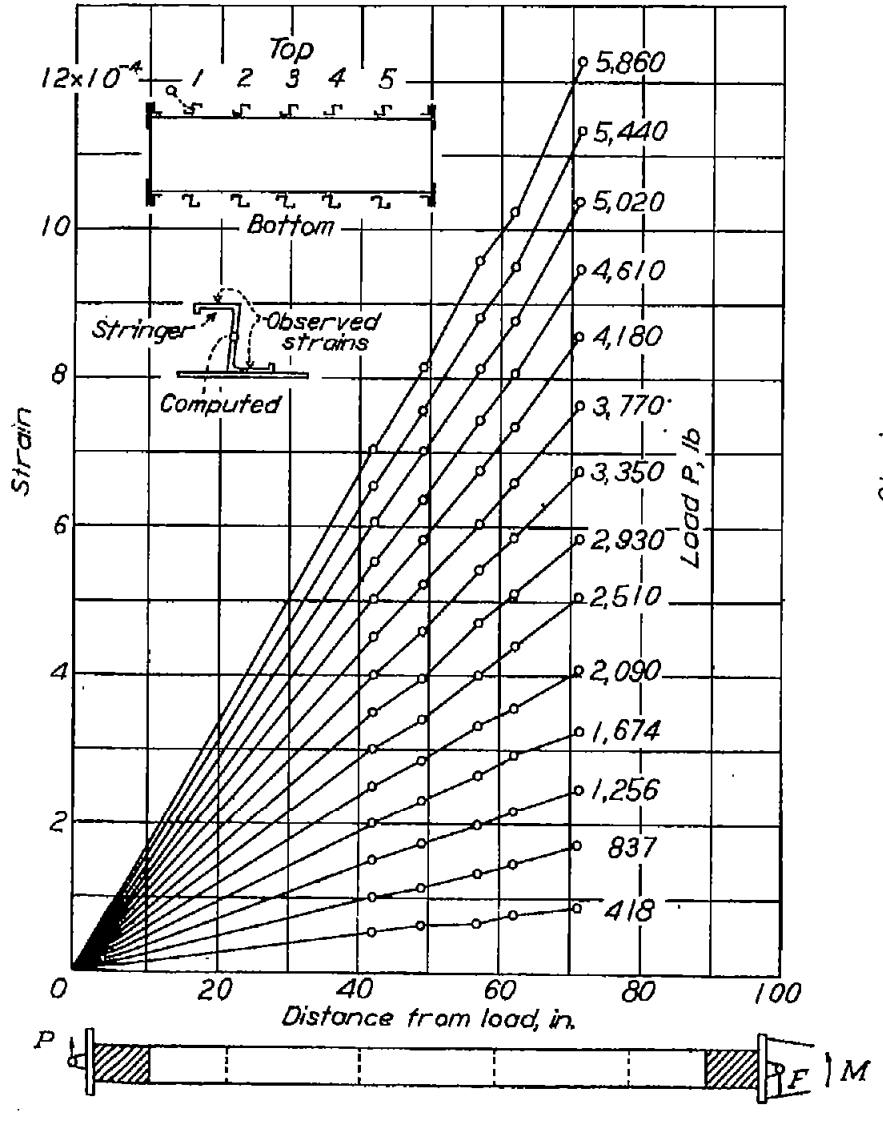

Figure 14.- Strains along centroid of top stringer 1.

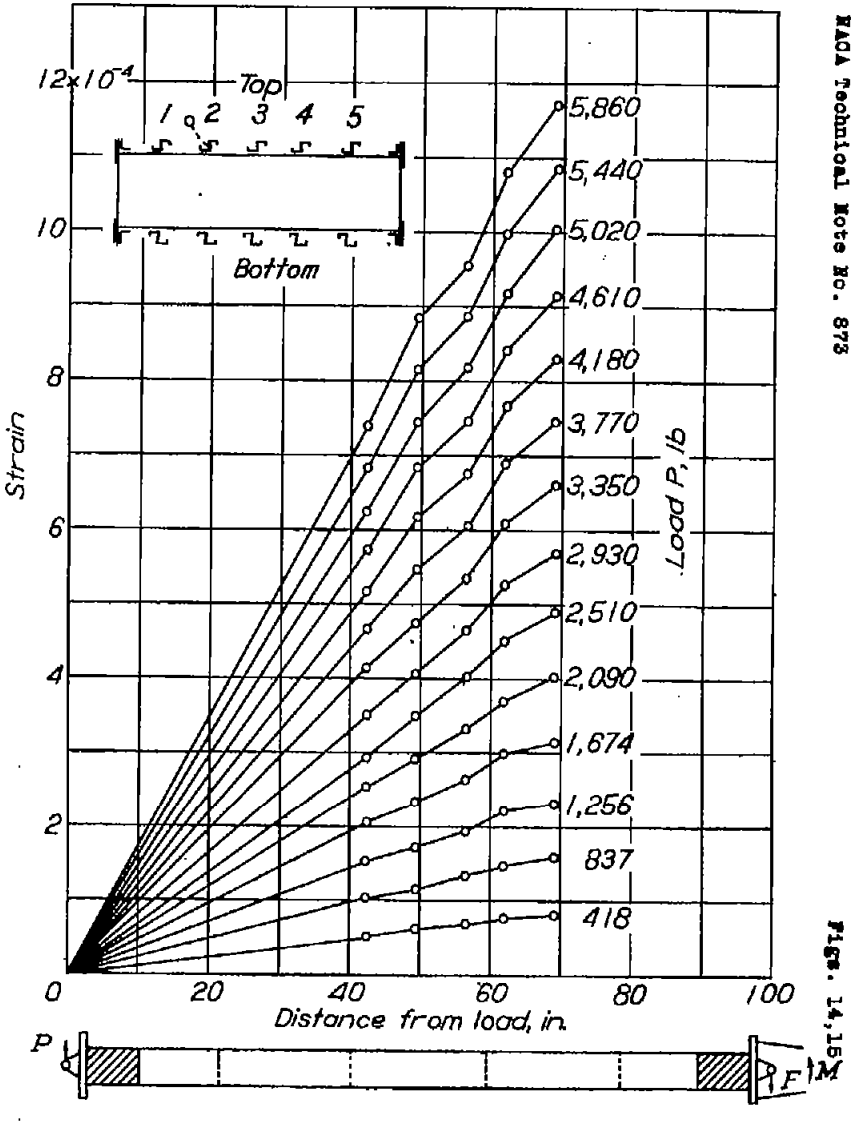

Figure 15.- Strains along centroid of top stringer 2.

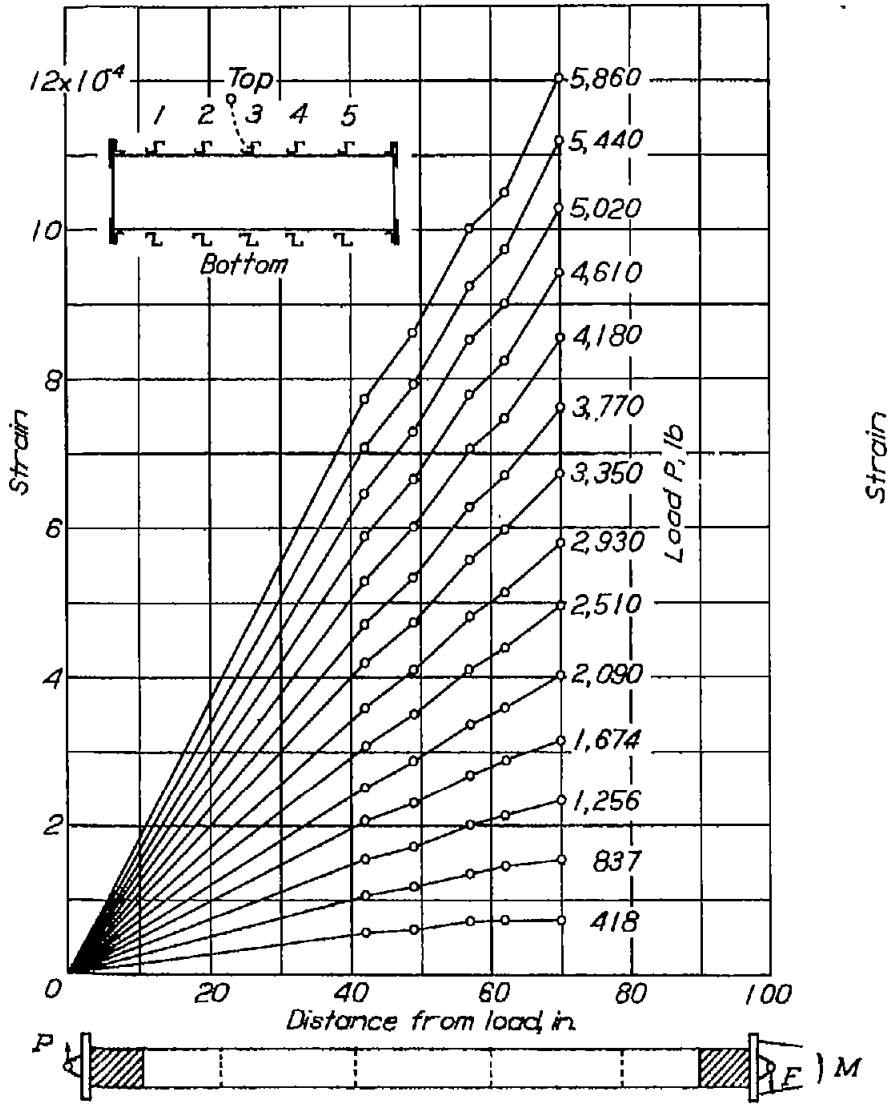

Figure 16.- Strains along centroid of top stringer 3.

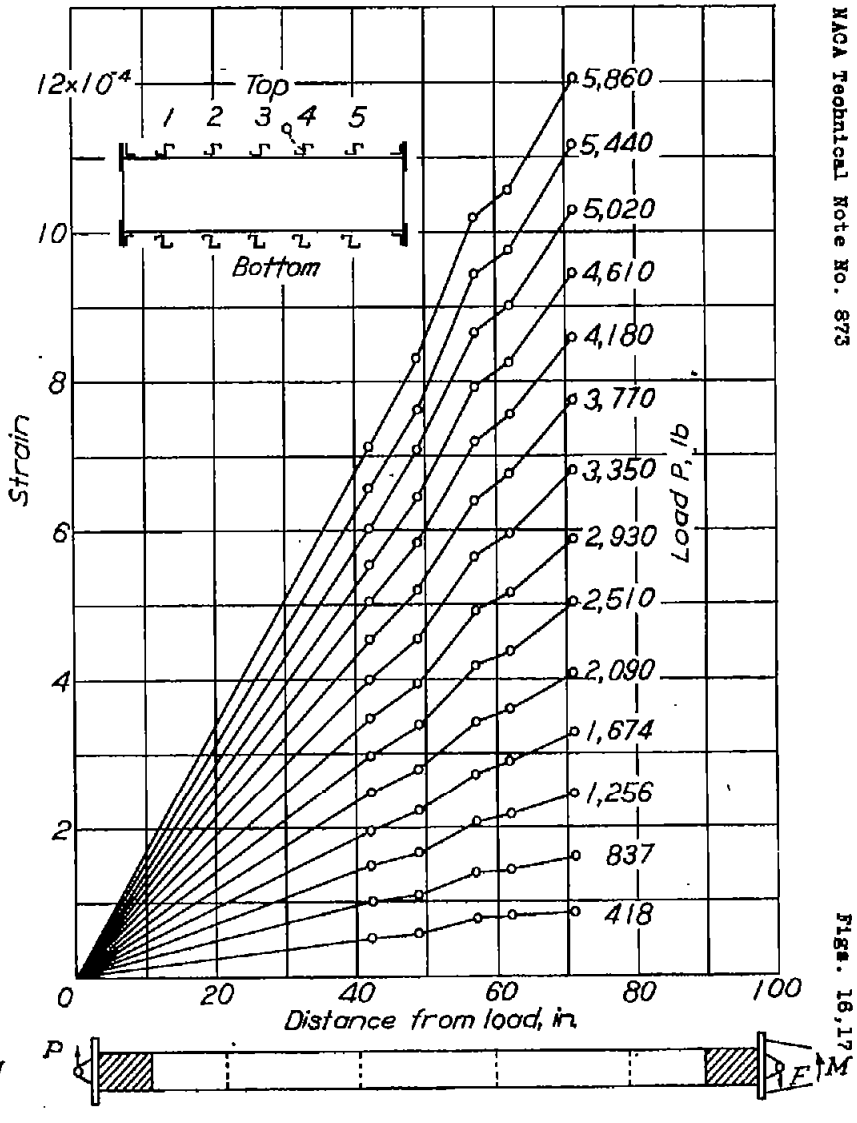

Figure 17.- Strains along centroid of top stringer 4.

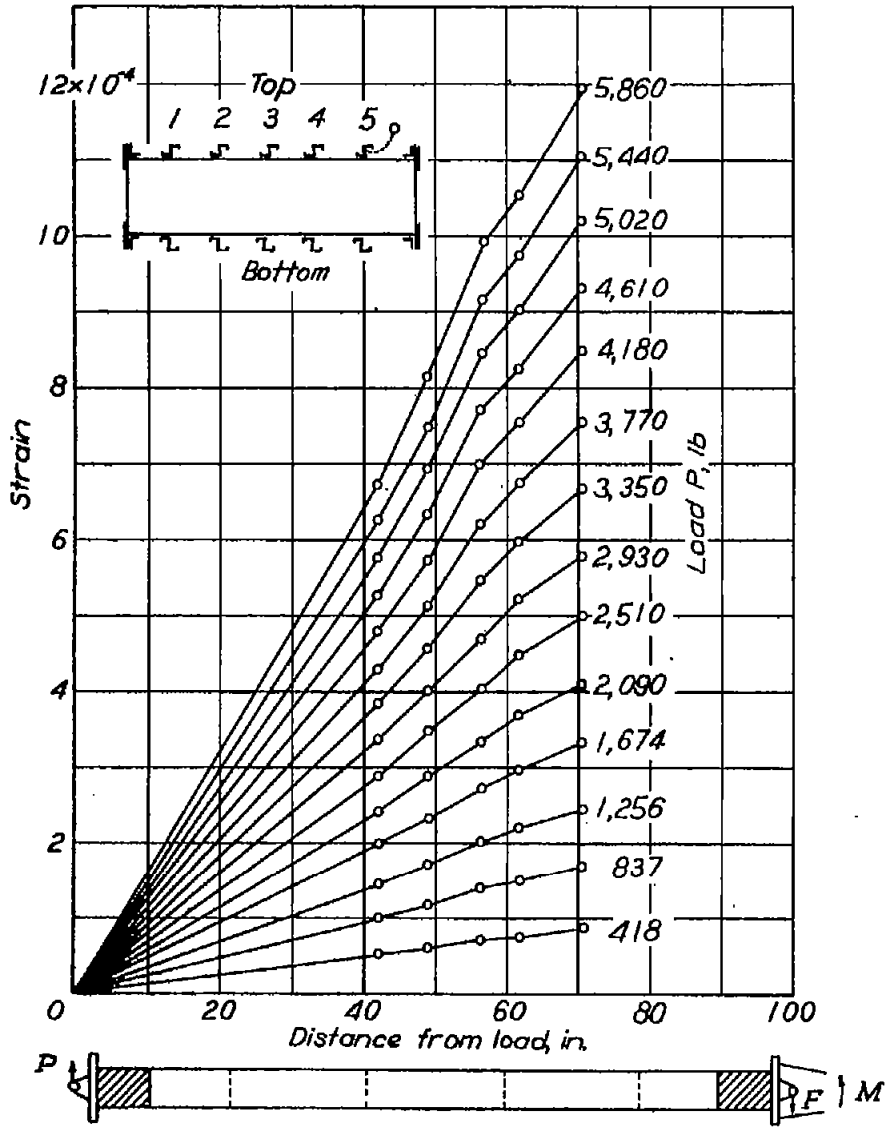

Figure 18.- Strains along centroid of top stringer 5.

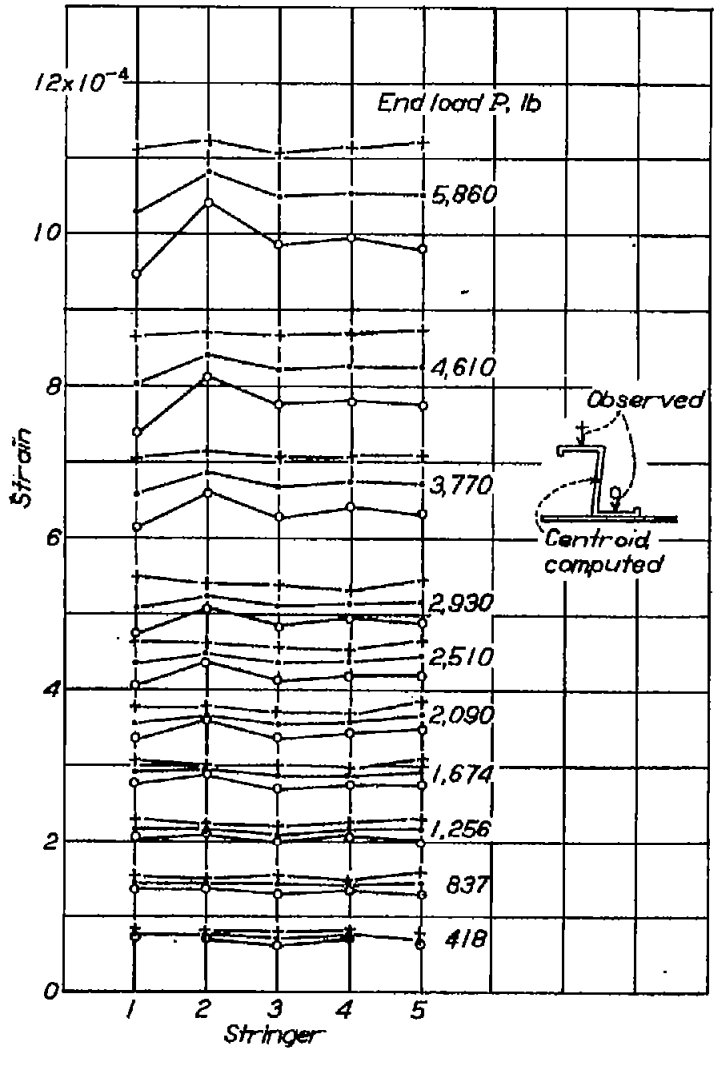

Figure 19.- Stringer strains (on top of box) at a section 62 inches from end load P, and near a bulkhead.

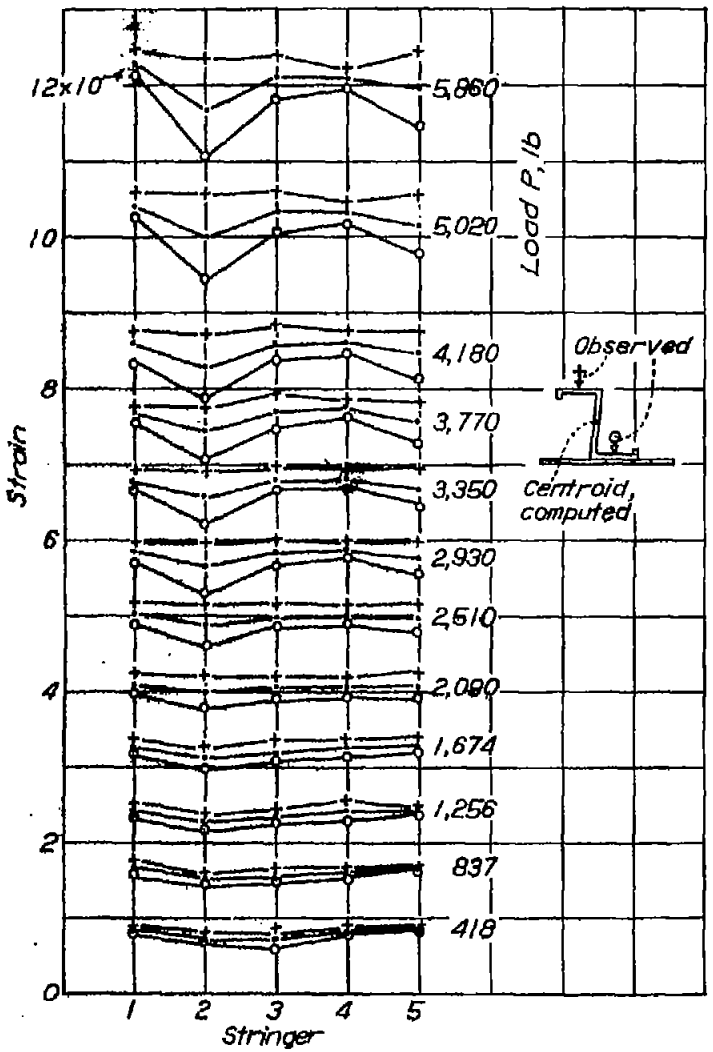

Figure 20.- Stringer strains (on top of box) at a section 70 inches from load and midway between bulkheads.

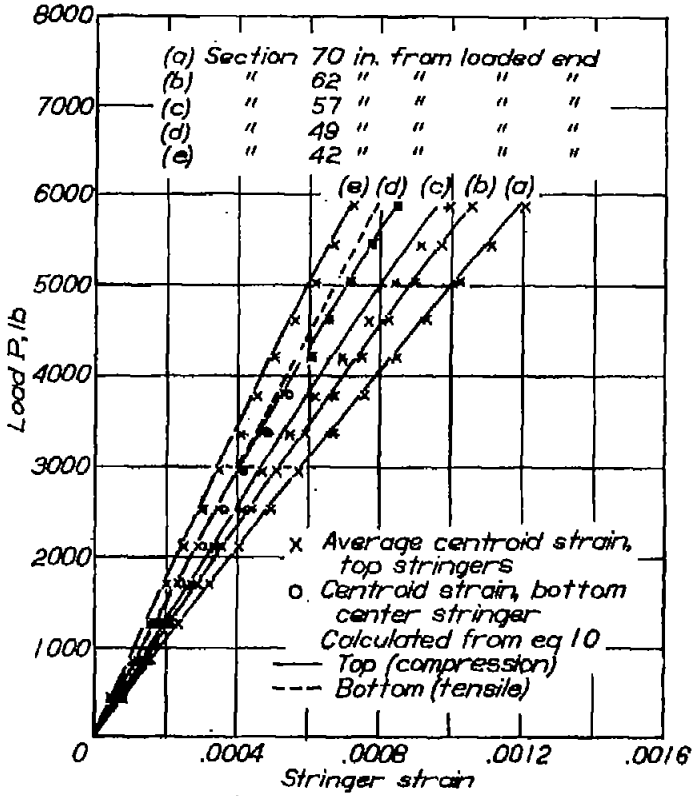

Figure 21.- Variation of load P with strain in stringers determined for various distances from loaded end.

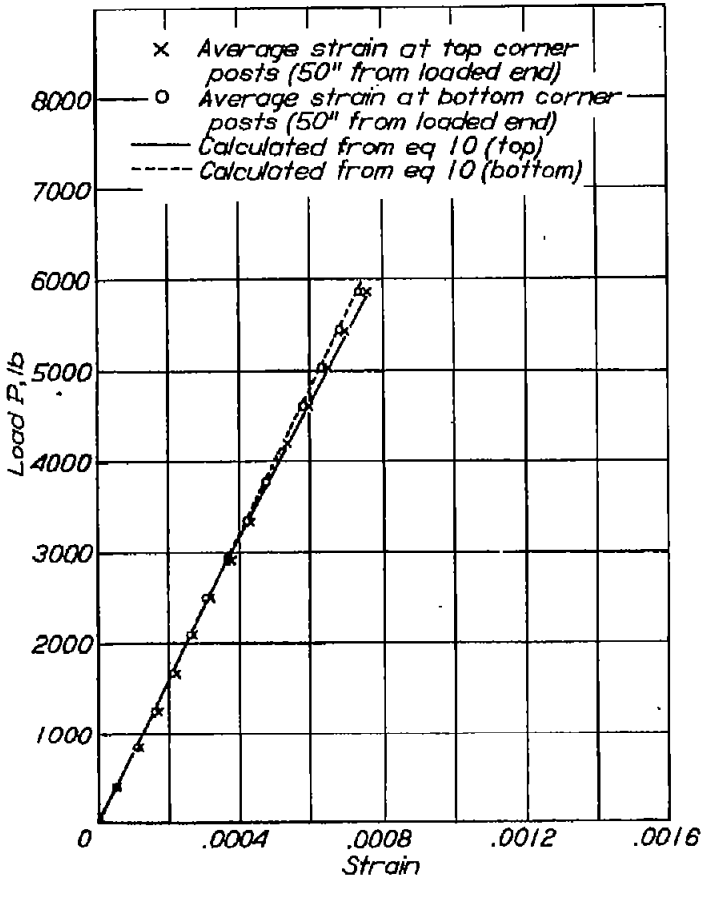

Figure 22.- Variation of load P with strain at corner posts at center section of beam.

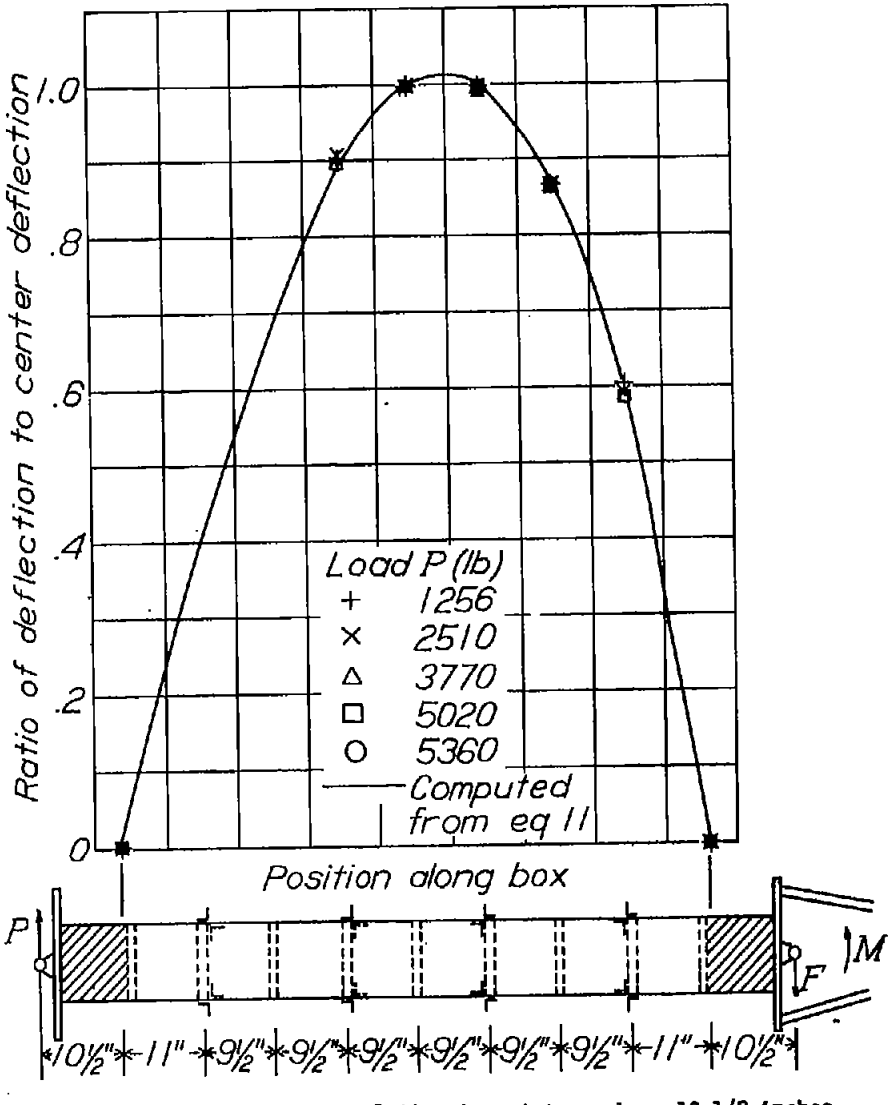

Figure 23.- Deflection curve relative to points on beam 10 1/2 inches from each end.

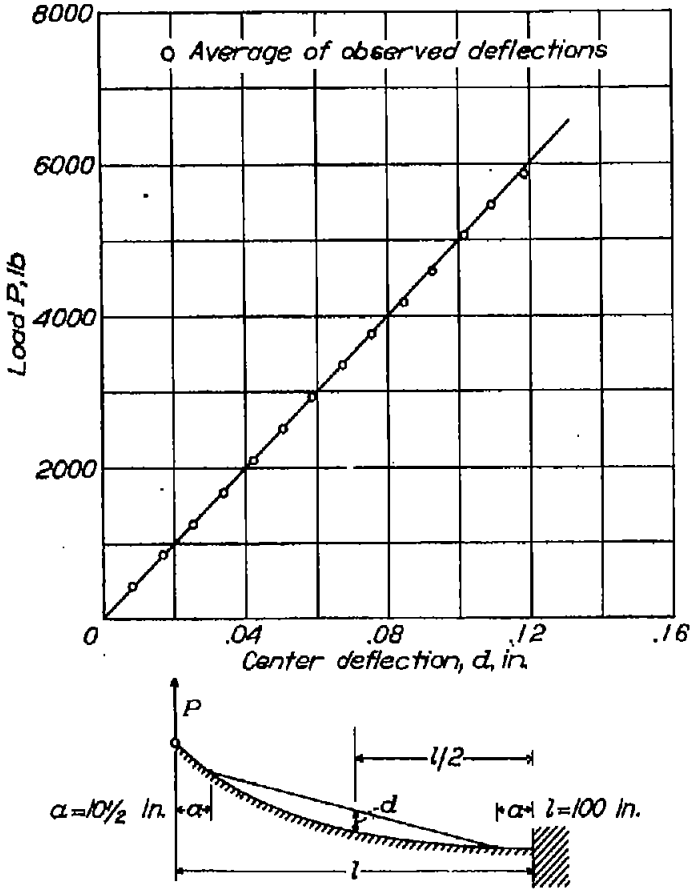

Figure 24.- Average of observed center deflections at two corner posts of box with respect to points 10 1/2 inches from the ends of the box.

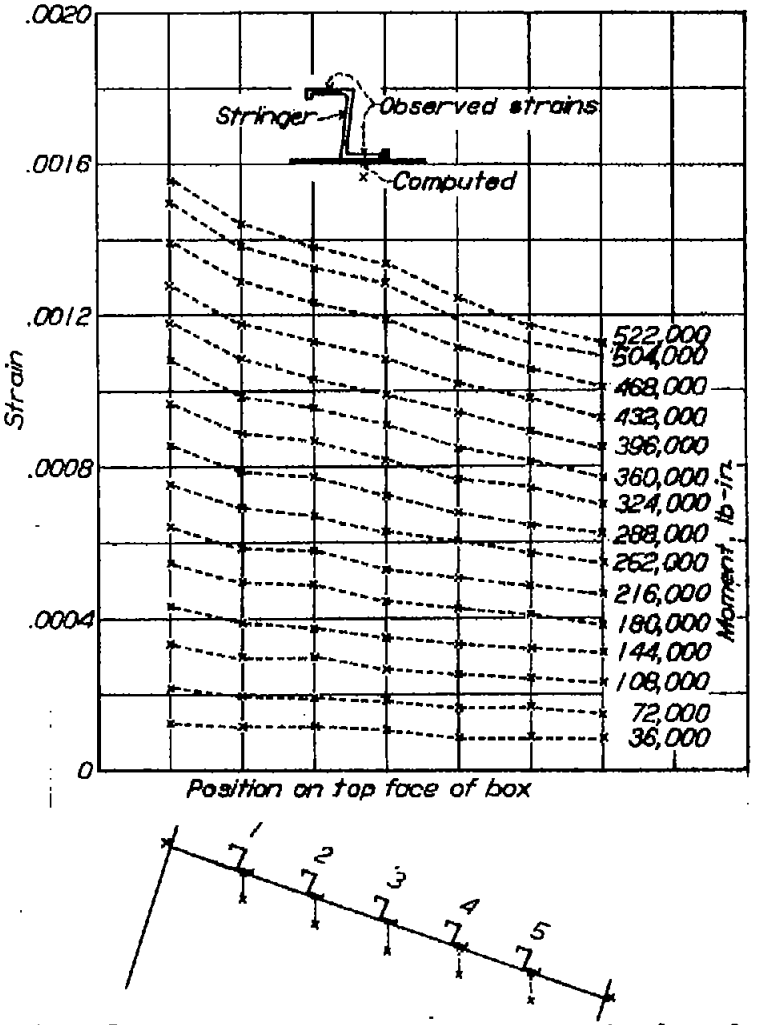

Figure 27.- Strain at center section on compression face of box for pure bending about both lift and drag axes.

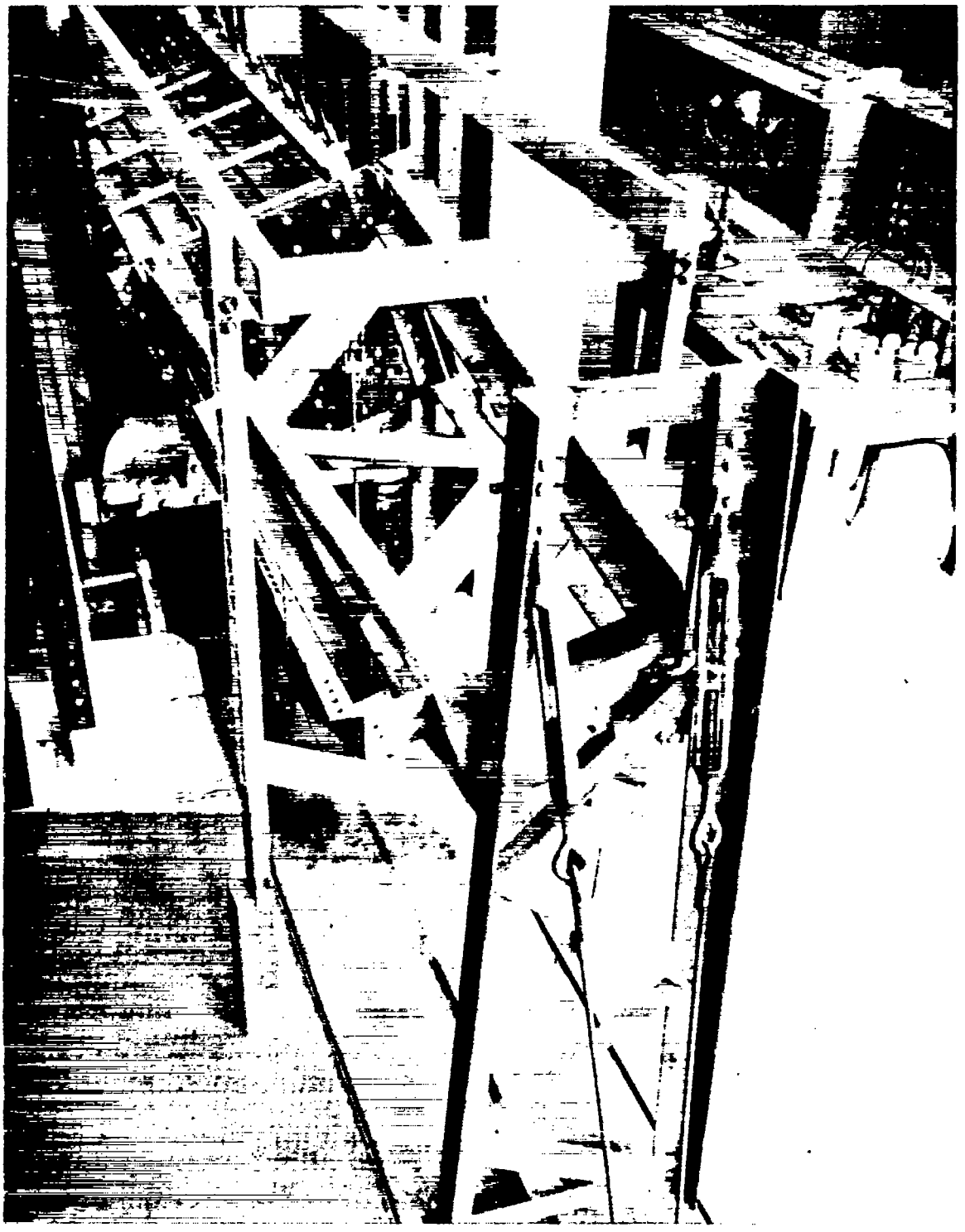

Figure 25.- Pure bending test about both lift and drag axes.

Figure 26.- Measurement of deflections and strains for pure bending about both lift and drag axes.

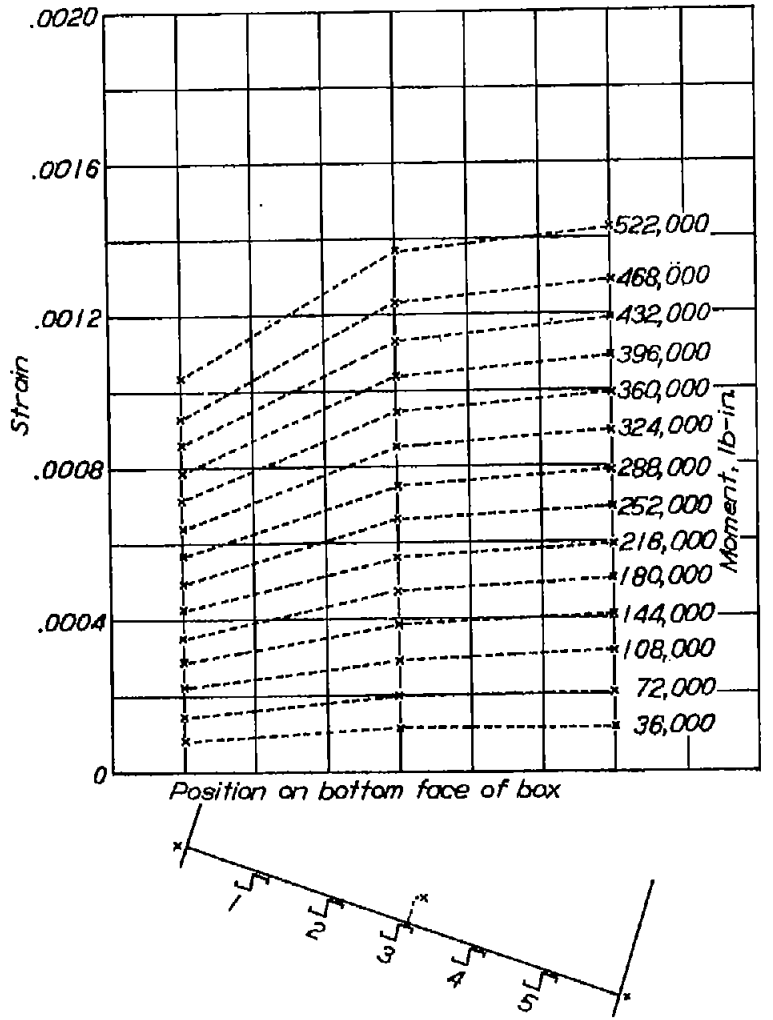

Figure 38.- Strain at center section on tension face of box for pure bending about both lift and drag axes.

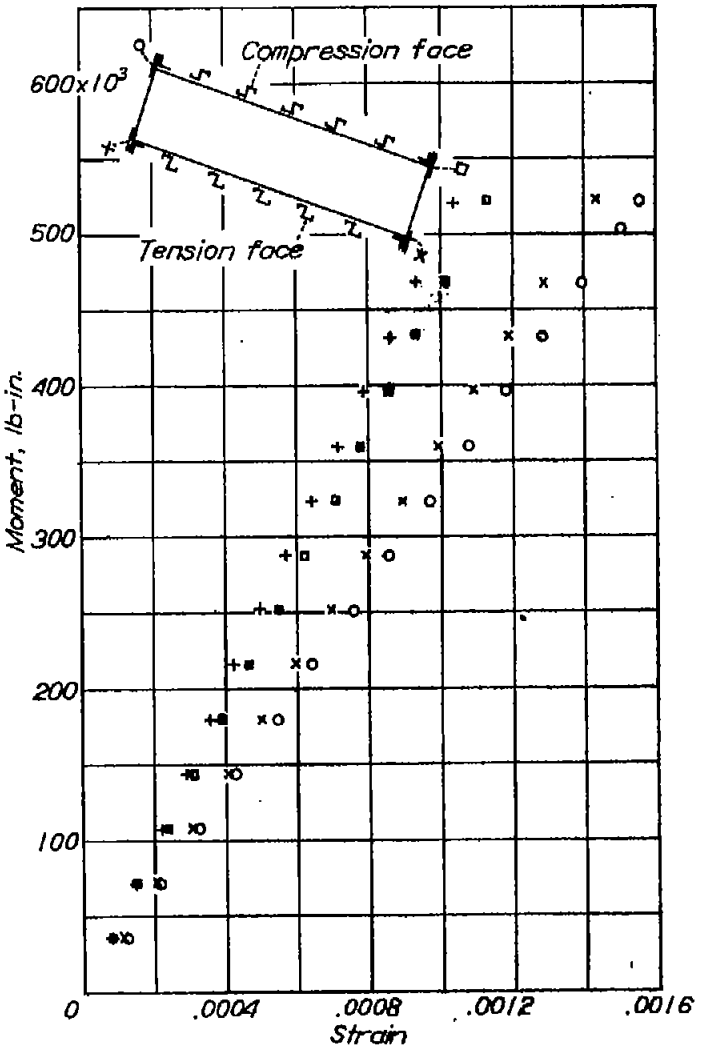

Figure 39.- Strain in corner posts at center section for box subjected to pure bending about both lift and drag axes.

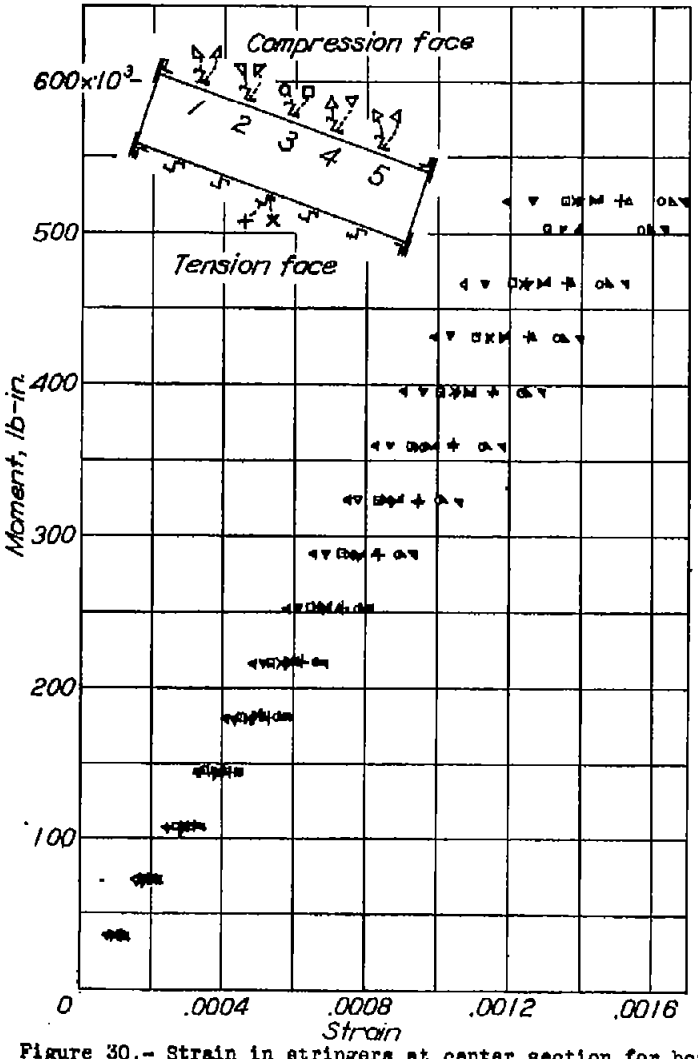

Figure 30.- Strain in stringers at center section for box subjected to pure bending about both lift and drag axes.

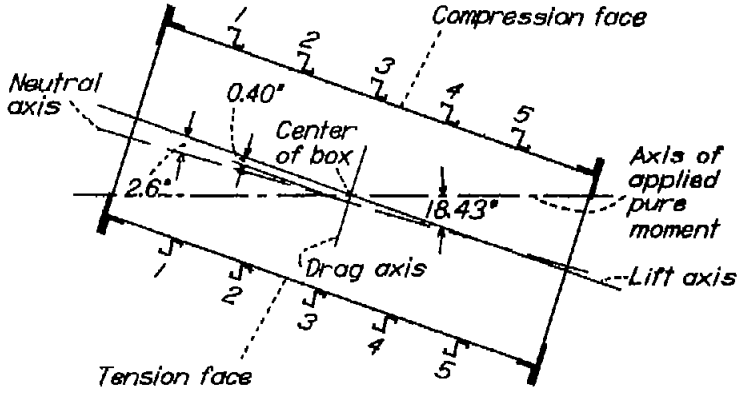

Figure 31.- Position of neutral axis at maximum applied moment (M = 522,000 lb-in.) for pure bending about both lift and drag axes.

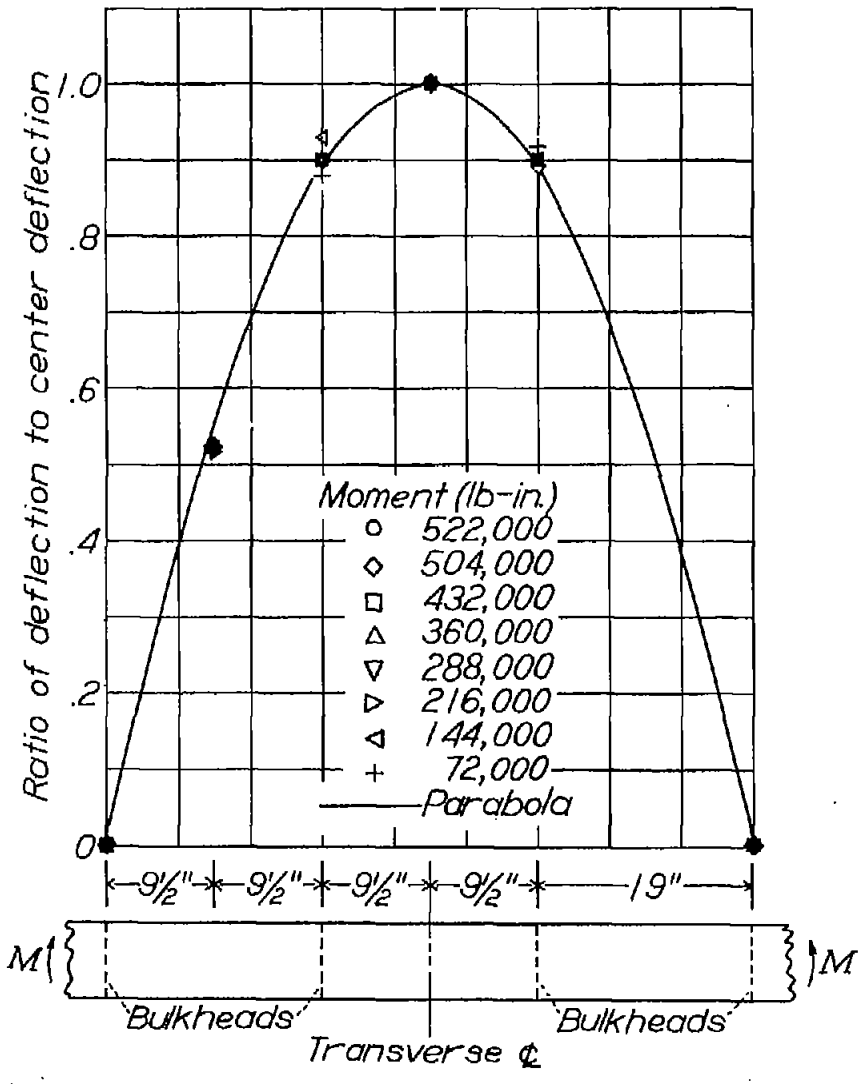

Figure 32.- Deflection curve normal to the lift axis for pure bending about both lift and drag axes.

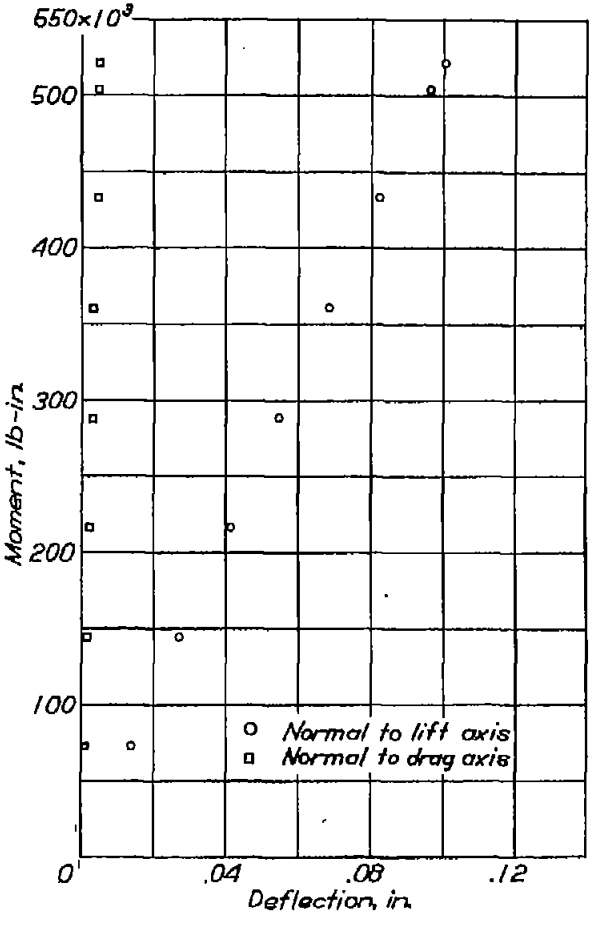

Figure 33.- Center deflections with respect to points 28.5 inches from each side of the transverse center line for pure bending about both lift and drag axes.

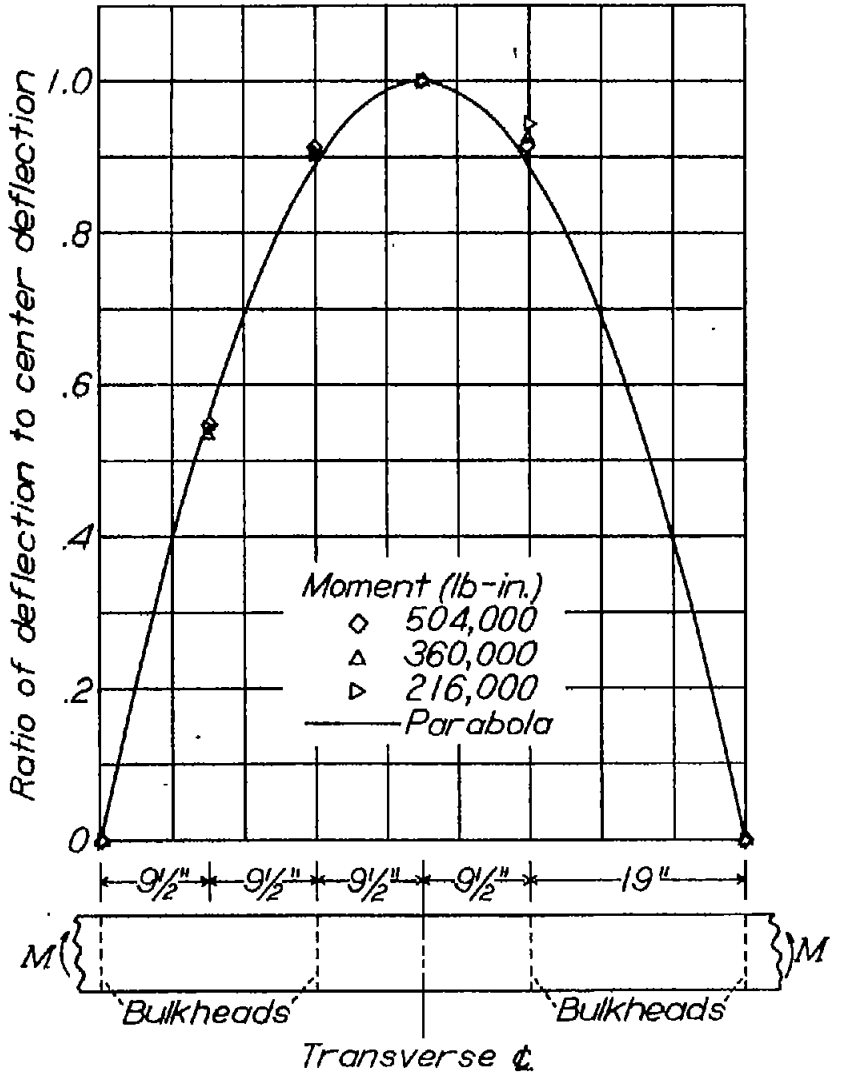

Figure 34.- Deflection curve normal to neutral axis for pure bending about both lift and drag axes.

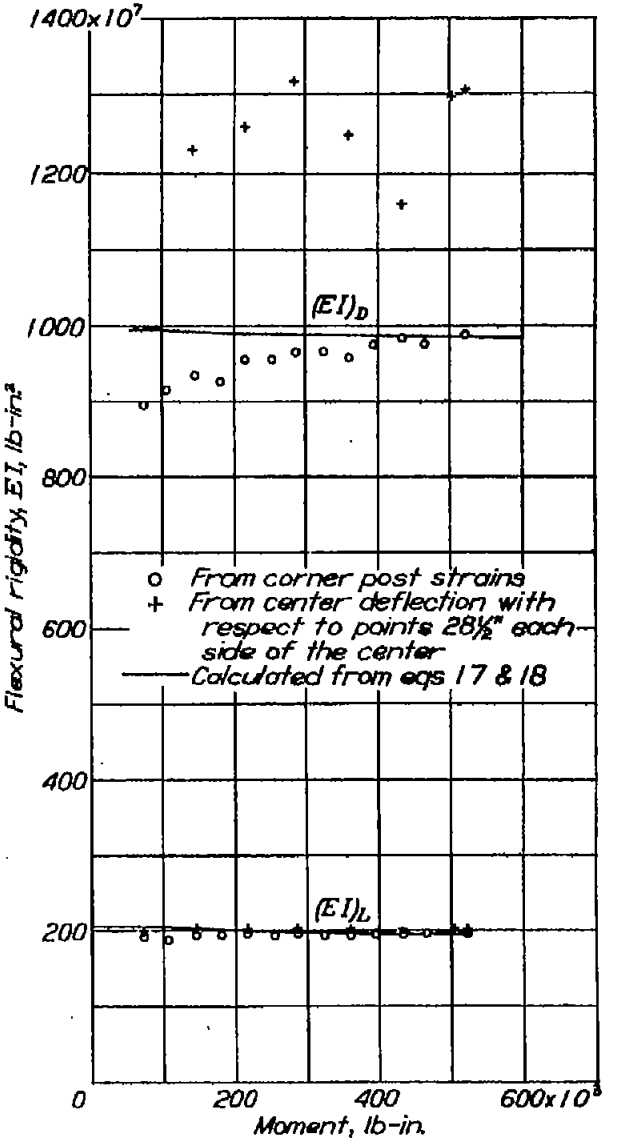

Figure 35.- Variation of effective flexural rigidity with moment for pure bending about both lift and drag axes.